



UWS Academic Portal

Development of Bi-polar plate design of PEM fuel cell using CFD techniques

Awotwe, Tabbi Wilberforce; El-Hassan, Zaki; Khatib, F. N.; Al Makky, Ahmed; Mooney, James; Barouaji, Ahmad; Carton, James; Olabi, Abdul-Ghani

Published in:
International Journal of Hydrogen Energy

DOI:
[10.1016/j.ijhydene.2017.08.093](https://doi.org/10.1016/j.ijhydene.2017.08.093)

Published: 05/10/2017

Document Version
Peer reviewed version

[Link to publication on the UWS Academic Portal](#)

Citation for published version (APA):
Awotwe, T. W., El-Hassan, Z., Khatib, F. N., Al Makky, A., Mooney, J., Barouaji, A., ... Olabi, A-G. (2017). Development of Bi-polar plate design of PEM fuel cell using CFD techniques. *International Journal of Hydrogen Energy*, 42(40), 25663-25685. <https://doi.org/10.1016/j.ijhydene.2017.08.093>

General rights

Copyright and moral rights for the publications made accessible in the UWS Academic Portal are retained by the authors and/or other copyright owners and it is a condition of accessing publications that users recognise and abide by the legal requirements associated with these rights.

Take down policy

If you believe that this document breaches copyright please contact pure@uws.ac.uk providing details, and we will remove access to the work immediately and investigate your claim.

Development of Bi-Polar Plate Design of PEM Fuel Cell Using CFD Techniques

Tabbi Wilberforce¹, Zaki El-Hassan¹, F.N. Khatib¹, Ahmed Al Makky¹, Jim Mooney¹, Ahmad Barouaji²,
James G. Carton³,
Abdul-Ghani Olabi¹

1. Institute of Engineering and Energy Technologies, University of the West of Scotland, UK.
2. School of Engineering, Faculty of Science and Engineering, University of Wolverhampton, UK.
3. School of Mechanical & Manufacturing Engineering, Dublin City University, Dublin, Ireland.

Abstract

This paper reviews the common existing designs of flow plates of fuel cells and suggests modifications to some of them to help reduce the pressure drop in the flow channels. Pressure drop is one of the factors that influence the overall performance of the cell both directly and indirectly through interaction with other factors including water management in the cell.

The work uses computational fluid dynamics (CFD) to examine different design and study the effect of varying the flow rate (i.e. velocity) on the pressure drop for each of the designs modelled. Again, the designs are optimized by changing different parameters using ANSYS CFX. Results showing the effects of the modifications on pressure drop in the various plates are presented in this paper.

From the study of the various designs, a conclusion was drawn that a modification of fuel cell designs in existence using a system similar to the diesel injection system design approach reduced the pressure drop in the fuel cell as shown by the simulation results.

This reduction in pressure drop will contribute to the improvement of performance but it must be stressed that other factors also contribute to the overall performance of the cell and reduction in pressure drop alone is not a guarantee of better performance of a certain fuel cell design.

Key words: Fuel Cell, Pressure Drop, CFD, Flow Plate, Mesh, Design Optimization.

Introduction

A fuel cell is any device that transforms chemical energy directly into an electrical energy and heat with high efficiency. They can also be described as batteries with flows of reactants in and

products out [1]. Fuel cells have quite a number of similarities with batteries but they differ in some aspects as well. They are all electrochemical devices that generate energy directly from electrochemical reaction between the fuel and the oxidant. Batteries are energy storing devices with their maximum energy available determined by the amount of chemical reactants stored in the battery. The reactants are usually built into the battery as well as being an energy conversion device. Recharging a secondary battery regenerates the reactants. This occurs when energy is being supplied to the battery. The fuel cell on the other hand is an energy conversion device that produces electrical energy for as long as the fuel and oxidant are continuously supplied to the electrodes [1].

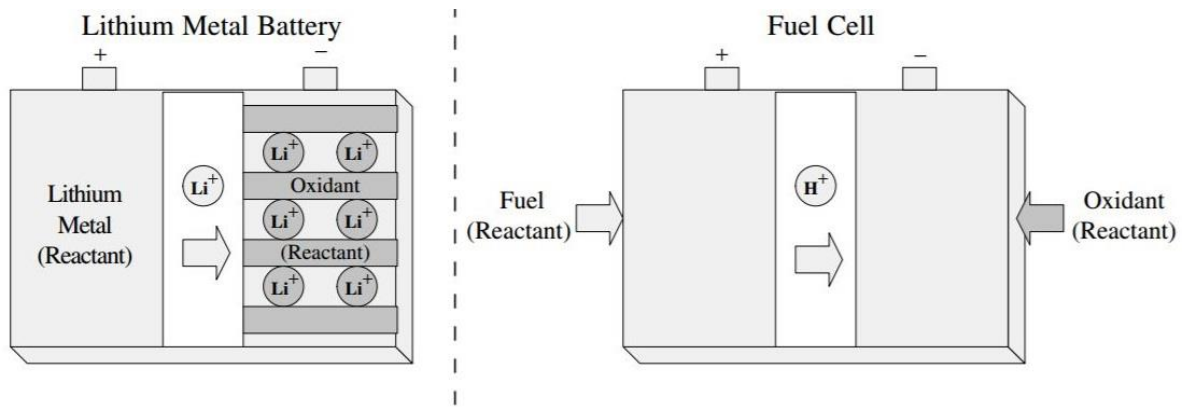


Fig. 1: Basic comparison between a Fuel cell and a Battery [2]

Primary batteries often have their lifetime being limited because once the chemical reactants stored in the battery runs out, the battery stops producing electricity. Again the lifetime of the battery is also limited as slow chemical reactions occur in the battery when it is even not in operation. A component in the battery that determines its life span is the electrode. This is because the electrodes are also consumed during the electrochemical reaction process. The reactants in fuel cells are often supplied in a continuous flow process and stored outside the fuel cell. When there is constant supply of the reactants, fuel cells will continue to produce electricity. Due to their sturdy and leak-proof construction, leakages do not usually occur in fuel cells to the same extent as in batteries. When the fuel cell is not in operation, there is very little possibility of corrosion occurring.

Comparing Fuel Cells to Heat Engines

The primary function of a heat engine is to convert chemical energy into electrical energy through intermediate steps. The process of combustion helps to first convert the chemical energy

into thermal energy. The next step is for the heat engine to convert the thermal energy into mechanical energy. The mechanical energy generated is then finally converted to electrical energy with the help of an electric generator. Normally several devices are needed to execute each step in order to finally generate the electricity. The maximum efficiency is limited by Carnot theorem because the conversion process is based on a heat engine that operates between low and high temperature. Moving parts are often involved in the process indicating possible irreversibilities leading to decreased efficiencies and equipment wear with time. Maintenance culture is highly important especially for the moving parts in order for the proper operation of the mechanical components [1].

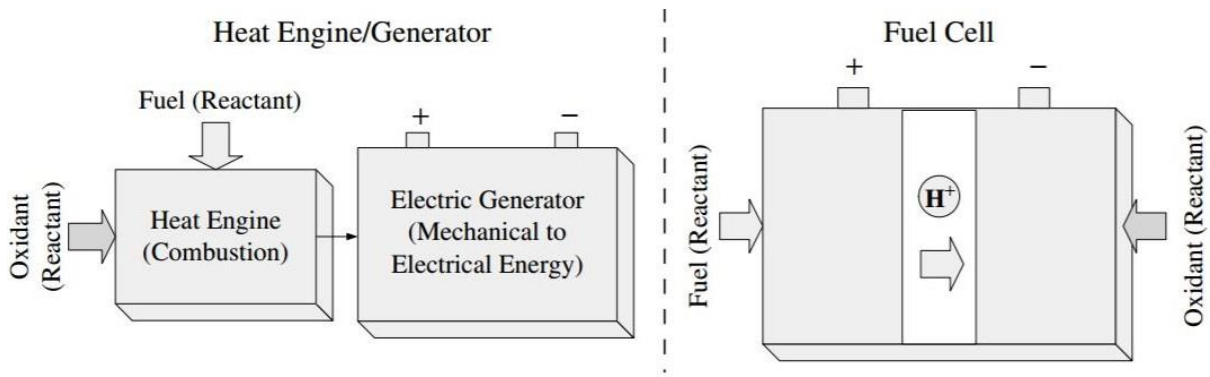


Fig. 2 Comparison between a fuel and Heat Engine/Generator [2]

Fuel cells do not have any moving parts hence their operations usually do not involve large irreversibilities, equipment's mechanical wear or unbearable noise. No moving parts mean they are highly reliable when in operation. Maintenance cost is equally reduced making them the best option for space and under water missions when long life is a priority. The electrochemical processes in fuel cells are not governed by the Carnot principles hence high operating temperatures are not necessary for achieving high efficiency. In addition, the efficiency of a fuel cell is not strongly dependent on the operating power. It is their inherent high efficiency that makes fuel cells an attractive option for a wide range of applications including road vehicle power sources, distributed electricity and heat production and portable systems [3].

Advantages and disadvantages of fuel cells

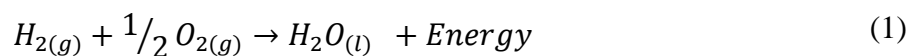
Fuel cells have the potential for a high operating efficiency that is not a strong function of system size. They also have a high scalable design with several types of fuel sources readily available.

Their environmentally friendly nature makes them the best of options in the energy generation industry as they produce zero or near zero greenhouse emissions [4]. Fuel cells have no moving parts hence very advantageous as there will be no wear, no vibrations and highly reliable operations in general. Fuel cells provide nearly instantaneous recharge capabilities when compared to batteries.

Unfortunately the advantages of fuel cells cannot be mentioned without considering their disadvantages as well. Some major limitations of fuel cell systems are costs, the need for mass produced pure hydrogen and its storage and delivery technology. In the event where pure fuel is not used, fuel reforming technology needs to be taken into account. If the fuels other than pure hydrogen are used, then fuel cell performance gradually decreases over time due to catalyst degradation and electrolyte poisoning [5]. Some types of fuel cells in existence are; Alkaline fuel cells (AFC), Direct Methanol fuel cells (DMFC), Phosphoric Acid Fuel cells and Proton Exchange Membrane (PEM) fuel cells. PEM fuel cells generally have very high efficiency and their impact on the environment is low as stated above. Possible use in transport as well as stationary and portable applications of fuel cell technology is a clear indication of the future of this useful energy generation medium.

Basic Operation of a fuel cell

The basic physical structure of a fuel cell consists of an electrolyte layer in contact with two porous electrodes with both electrodes containing catalysts to speed up the electrochemical processes. One electrode is negatively charged (anode) and the other electrode is positively charged (cathode) as is shown in Fig. 1. Electrochemical reactions take place at the electrodes to produce an electric current. The basic operation of the hydrogen fuel cell is the reverse situation of the process of the electrolysis; the hydrogen and oxygen are recombining, and an electric current is produced along with the water obtained. The overall reaction is described in the following equation:



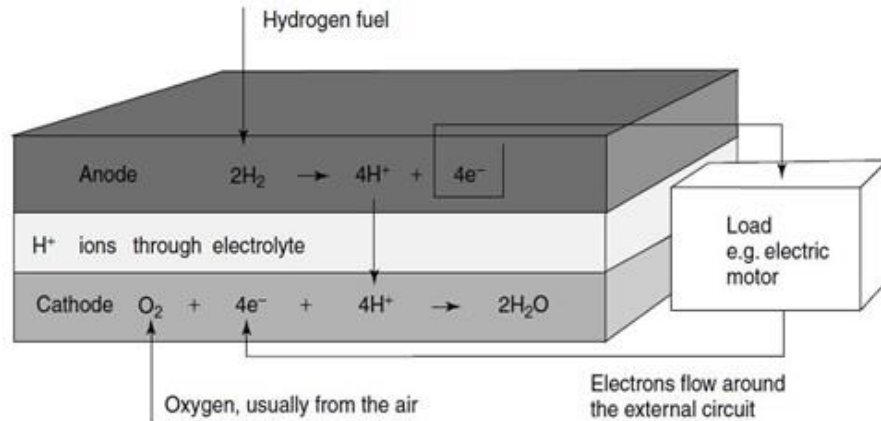


Fig. 3: Acid electrolyte fuel cell scheme [5]

It is possible to distinguish two main categories of fuel cells depending on the kind of electrolyte used: acid electrolyte fuel cells and alkaline electrolyte fuel cells. In both types the overall reaction is the same as shown in Eqn. 1, but the half reactions at each electrode are different. The main difference between them is the charge carrier: a positive one for the first type, and a negative one for the second type. At the anode of the acid electrolyte fuel cell the hydrogen gas ionises releasing electrons and H^+ ions (protons), while at the cathode oxygen reacts with electrons arriving through the external circuit and H^+ ions that are passing through the electrolyte to form water. On the other hand in the alkaline electrolyte fuel cell, hydroxyl ions (OH^-) are made at the cathode and then they react at the anode with hydrogen releasing electricity and producing water. At the cathode, oxygen reacts with electrons to produce new hydroxyl (OH^-) ions. Similarly in the alkaline electrolyte fuel cells to allow these reactions to proceed continuously, the ions must be able to pass through the electrolyte while the electrons pass from the anode to the cathode through the electric circuit [6].

Table 1 shows the different half-reactions for both alkaline and acid fuel cells.

TABLE 1. HALF REACTIONS OF ACID AND BASIC ELECTROLYTE FUEL CELLS (4)

	Acid electrolyte	Basic electrolyte
Anode reaction	$H_2 \rightarrow 2H^+ + 2e^-$	$H_2 + 2OH^- \rightarrow 2H_2O + 2e^-$
Cathode reaction	$\frac{1}{2}O_2 + 2H^+ + 2e^- \rightarrow H_2O$	$\frac{1}{2}O_2 + H_2O + 2e^- \rightarrow 2OH^-$
Overall reaction	$H_2 + \frac{1}{2}O_2 \rightarrow H_2O$	$H_2 + \frac{1}{2}O_2 \rightarrow H_2O$

Fuel cells can also be categorized into different types based on the type of the reactant used (e.g. hydrogen, methanol, methane, carbon monoxide and other organic substances, etc.); the electrolyte type (acid or alkali, liquid or solid), and the operating temperature (low-temperature fuel cells (120°C-150°C), intermediate temperature fuel cells (150°C-250°C), interim-temperature fuel cells (250°C-650°C) and high-temperature fuel cells (over 650°C) [7]).

An overview of the main 14 different types of fuel cells has been made, and the main features are shown in Table 2 and Table 3.

TABLE 2. MAIN FEATURES OF DIFFERENT TYPES OF FUEL CELLS: FUEL, CATALYST AND ELECTROLYTE (4)

	Fuel	Catalyst	Electrolyte
Low-Temperature Proton Exchange Membrane Fuel Cells (LT-PEMFCs)	Hydrogen (H ₂)	Platinum supported on carbon	Solid polymer membrane (Nafion)
High-Temperature Proton Exchange Membrane Fuel Cells (HT-PEMFCs)		Platinum-Ruthenium supported on carbon	Nafion/PBI doped in phosphoric acid
Phosphoric Acid Fuel Cells (PAFCs)	Hydrogen (H ₂)	Platinum supported on carbon	Liquid phosphoric acid (H ₃ PO ₄) in silicon carbide (SiC)
Direct Methanol Fuel Cells (DMFCs)	Liquid methanol-water solution	Platinum/Platinum-Ruthenium supported on carbon	Solid polymer membrane (Nafion)
Direct Ethanol Fuel Cells (DEFCs)	Liquid ethanol-water solution	Platinum/Platinum-Ruthenium supported on carbon	Solid Nafion/Alkaline media/Alkaline-acid media
Alkaline Fuel Cells (AFCs)	Hydrogen (H ₂)	Nickel/Silver supported on carbon	Potassium hydroxide (KOH) in water solution/Anion exchange membrane (AEM)
Molten Carbonate Fuel Cells (MCFCs)	Methane	Nickel Chromium (NiCr)/Lithiated nickel (NiO)	Liquid alkali carbonate (Li ₂ CO ₃ /Na ₂ CO ₃ /K ₂ CO ₃) in Lithium aluminate (LiAlO ₂)
Solid Oxide Fuel Cells (SOFCs)	Methane	Nickel-YSZ composite/Strontium-doped lanthanum manganite (LSM)	Solid yttria-stabilized zirconia (YSZ)
Proton Ceramic Fuel Cells (PCFCs)	Methane	Nickel	Protonic/Zirconia
Zinc-Air Fuel Cells (ZAFCs)	Zinc	Non-noble metal oxides (such as manganese oxide - MnO ₂)	Liquid alkalines

Direct Borohydride Fuel Cells (DBFCs)	Sodium borohydride (NaBH ₄)	Gold/Silver/Nickel/Platinum supported on carbon	Solid Nafion/Anion exchange membrane (AEM)
Direct Formic Acid Fuel Cells (DFAFCs)	Liquid formic acid (HCOOH)	Palladium/Platinum supported on carbon	Solid Nafion
Direct Carbon Fuel Cells (DCFCs)	Solid carbon (coal, coke, biomass)	Graphite or carbon-based material/Strontium-doped lanthanum manganite (LSM)	Solid yttria-stabilized zirconia (YSZ)/Molten carbonate/Molten hydroxide
Enzymatic Fuel Cells (BFCs)	Organic matters (glucose)	Biocatalyst supported on carbon	Ion exchange Membrane/Membrane-less
Microbial Fuel Cells (BFCs)	Any organic matter (glucose, acetate, wastewater)	Biocatalyst supported on carbon/Platinum supported on carbon	Ion exchange Membrane

TABLE 3. MAIN FEATURES OF DIFFERENT TYPES OF FUEL CELLS: ELECTRICAL EFFICIENCY, OPERATING TEMPERATURE AND CHARGE CARRIER (4)

	Electrical efficiency	Operating Temperature	Charge carrier
Low-Temperature Proton Exchange Membrane Fuel Cells (LT-PEMFCs)	40% - 60%	60°C - 80°C	Hydrogen Ion (H ⁺) (proton)
High-Temperature Proton Exchange Membrane Fuel Cells (HT-PEMFCs)	50% - 60%	110°C-180°C	
Phosphoric Acid Fuel Cells (PAFCs)	36% - 45 % (85% with cogeneration)	160°C - 220°C	Hydrogen ion (H ⁺) (proton)
Direct Methanol Fuel Cells (DMFCs)	35% - 60%	Ambient - 110°C	Hydrogen Ion (H ⁺) (proton)
Direct Ethanol Fuel Cells (DEFCs)	20% - 40%	Ambient - 120°C	Hydrogen ion (H ⁺) (proton)

Alkaline Fuel Cells (AFCs)	60-70 %	Below zero - 230°C	Hydroxyl ion (OH)-
Molten Carbonate Fuel Cells (MCFCs)	55% - 65% (85% with cogeneration)	600°C-700°C	Carbonate ion (CO ₃) ²⁻
Solid Oxide Fuel Cells (SOFCs)	55% - 65% (85 % with cogeneration)	800°C – 1000°C	Oxygen Ion (O ₂ -)
Proton Ceramic Fuel Cells (PCFCs)	55% - 65%	700°C – 750°C	Hydrogen ion (H ⁺) (proton)
Zinc-Air Fuel Cells (ZAFCs)	30% - 50 %	Below zero – 60°C	Hydroxyl ion (OH)-
Direct Borohydride Fuel Cells (DBFCs)	40% - 50%	20°C – 85°C	Sodium ion (Na ⁺)
Direct Formic Acid Fuel Cells (DFAFCs)	30% - 50%	30°C – 60°C	Hydrogen ion (H ⁺) (proton)
Direct Carbon Fuel Cells (DCFCs)	70% - 90%	600°C – 1000°C	Oxygen Ion (O ₂ -)
Enzymatic Fuel Cells (BFCs)	30%	20°C – 40°C	Hydrogen ion (H ⁺) (proton)
Microbial Fuel Cells (BFCs)	15% - 65%	20°C – 60°C	

Principle of Operation of the Proton Exchange Membrane fuel cell

PEM fuel cell operates based on the principles of electrochemical reactions between hydrogen (fuel) and Oxygen from air (oxidant) in the presence of a platinum catalyst [8]. Hydrogen fuel is transported through field flow plates to the anode on one side of the cell while air provides oxygen to the cathode on the other side of the cell. Once the hydrogen reaches the catalyst active sites on the anode side, it breaks into positive hydrogen ions (protons) and negatively charged electrons. The electrons and positively charged protons react with the oxygen at the cathode forming water. The outlet serves as the exit for some of the water. Flooding of the fuel cell

occurs when some of the water generated remains in the fuel cell due to their inability to exit the cell [9]. A schematic representation of a fuel cell with reactant/product gases and ion conduction flow directions through the fuel cell is shown in Fig (4) and Fig (5).

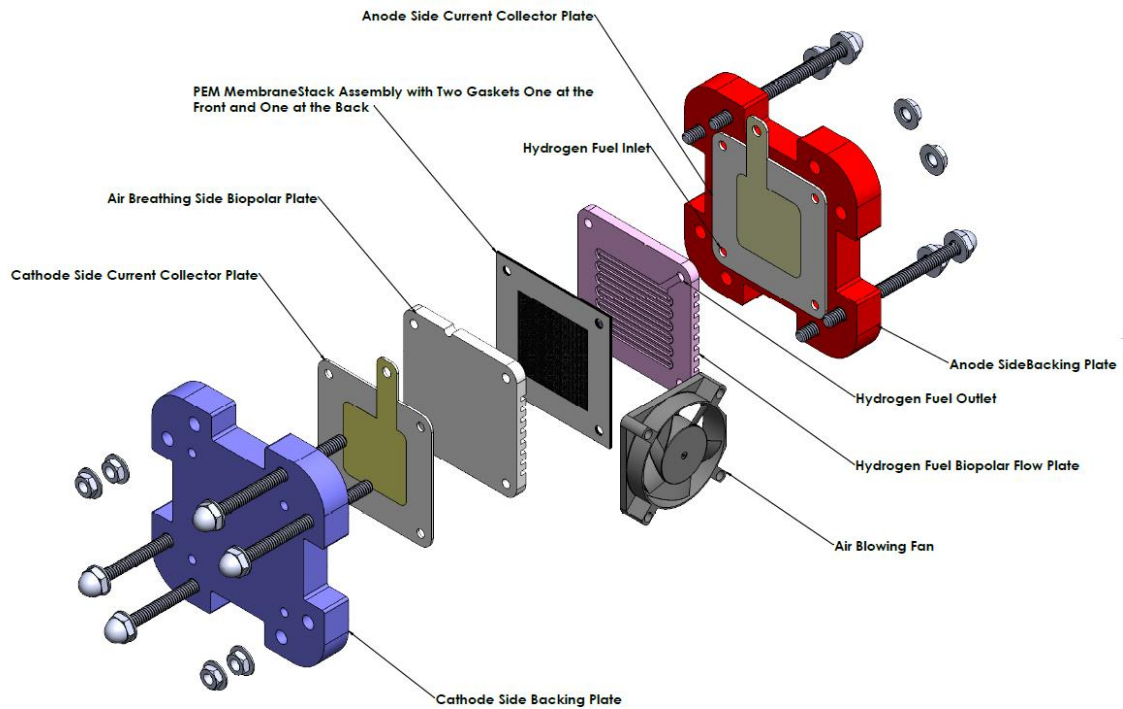


Fig. 4: Exploded View of a Proton Exchange Membrane fuel cell.

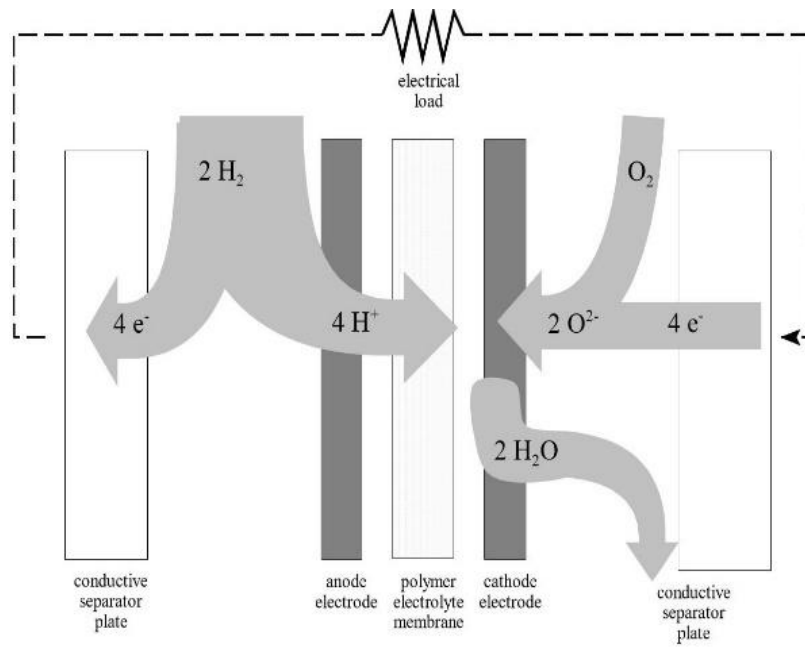


Fig. 5 Schematic Diagram of PEM fuel cell [8]

The polymer membrane electrolyte allows only positive ions to pass through it to the cathode. The negatively charged electrons then travels through an external circuit to the cathode, creating an electric current [10, 11]. Membrane Electrode Assembly (MEA) and bipolar plates remain the main component of PEM fuel cell. While the MEA serves as the platform for chemical reaction to occur in the fuel cell, the bipolar plates take care of the transport of reactants (fuel and oxidant) to the reactive sites of the MEA. This process immensely affects the general performance of the fuel cell. Efficient distribution of fuel and the oxidant to the catalyst layer, can increase the utilization of the catalyst, improve the water management through the cell and provide effective collection of the produced current [12]. The MEA is made up of Proton Exchange Membrane, an electrically conductive porous Gas diffusion layer (GDL) and an electro-catalyst layer sandwiched between two flow plates. Graphite in recent times has been the common used bipolar plates in fuel cells but they have weak mechanical strength and also generally brittle. They are also expensive to machine [13]. Bipolar plates account for nearly 70% of the volume and weight of the fuel cell stack. It also contributes to about 40% of the cost of the fuel cell stack [13,14]. Metallic plates have recently arisen as the plate of choice for bipolar plates. Low cost, easy to process, good mechanical strength, good electrical and thermal conductivities are some of the advantages of using metallic plates. For effective distribution of reactants evenly and better utilize the whole of MEA, flow channels are often machined on the surfaces of the bipolar plates. These channels could be parallel, serpentine, pins, straight or interdigitated [15-18]. Recent studies conducted by a number of researchers show that the flow field design significantly affects the cell performance [19 - 25]. Poorly designed flow field can cause inefficient water removal and hinder reactant transport. Manso et al [26] did a detailed review on all the common types of flow plates and some of the drawback they identified was large pressure losses, high cost of manufacturing and low mechanical strength resulting in thicker plates which increase the weight and volume of the fuel cell. The flow channel(s) can also lead to uneven distribution of the electrochemical reactants, which lead to irregular utilization of the catalyst [27]. Open pore cellular foam (OPCF) material has recently been used by a number of researchers around the world as alternative to the traditional flow field design [28]. These open pore cellular foams provide better gas distribution throughout the fuel cell and also there is pressure drop between the inlet and outlet [28, 29]. Using carbon foams as the gas flow field has also been investigated [30]. Other researchers also reported in their findings that

flow field(s) with metal foam has impact on the performance of the PEM fuel cell [31]. They thoroughly investigated the effect of the flow field designs on the performance of a PEM fuel cell. They concluded that the flow field can play an active role in the design and development of PEM fuel cells with either conventional or foam flow plates. Kumar and Reddy [32, 33] used foam material in place of the channels of conventional flow plates. This retrofitting of a flow plate is crude and will not allow the full benefits of OPCF materials to be exploited. With all these advantages of using the OPCF, researchers still face challenges in relation to the housing unit where the foam will be placed. This paper seeks to investigate a new housing unit for the OPCF material and the data gathered about pressures, flow regimes and velocity profiles will be analysed.

In conventional flow plates, the flow behaviour of oxygen and hydrogen inside the fuel cell and through the flow plates can be effectively predicted and analysed by employing Computational Fluid Dynamic (CFD) modelling tools and many researchers [34-36] employed CFD tools in their studies to develop and optimize the bipolar flow plates.

Modelling and Simulations

ANSYS, Inc. is an engineering simulation software (computer aided engineering or CAE) developer that makes use of CFD, FEM and some various types of programming algorithms for simulation and optimization. Any project simulation conducted in ANSYS involves five steps for the completion of the project (geometry creation, meshing, simulation setup, running the calculations and post processing).

CFD programs are often used to predict the flow patterns and regimes, velocity profiles, and pressure gradients in parts of the fuel cell components or through the full flow plates and flow fields. The flow plates used in this study are designed to cover an active area of 25cm². This is basically the active area being used by the fuel cell. Some of the key parameters which are very necessary to consider when designing a flow plate channel layout are the distribution of pressure on the GDL and membrane, pressure drop in and through the flow plate, distribution of temperature on the GDL and membrane, consistent reactant concentration over the whole active area of the GDL and membrane, membrane hydration and mitigation of flooding.

Meshing Dependence

One of the key steps in the CFD simulation process is the creation of the mesh. The collection of differential and algebraic equations that describe the process are solved (approximated) using different techniques at these mesh elements. The meshing process breaks the domain in small entities that constitute the mesh.

For a valid CFD simulation, the results obtained need to be independent of the mesh size or the type of elements used and convergence studies are necessary to ensure this.

The size of the mesh and grid elements types can be modified by using the controls of the meshing engine of ANSYS.

In this study and since the channels are mostly straight, a representative element is used to carry out the convergence studies.

Simulations were run to examine the dependency of the pressure drop results on the mesh for several values of the gas flow velocity in the straight representative channel.

Mesh 1

The first mesh tried was done for a channel like design which was 100mm in length and 20 mm in width with appropriate thickness. The mesh as shown in Fig. 6 was created using automatic meshing method. The size function was set to proximity and curvature and the relevance centre was left at the coarse setting. The transition was set to slow. These setting resulted in 1,760 nodes and 1,161 elements.

Figs. 7a and 7b show the velocity profile and pressure drop for the mesh through the horizontal channel depicting the porous fluid domain in the fuel cell

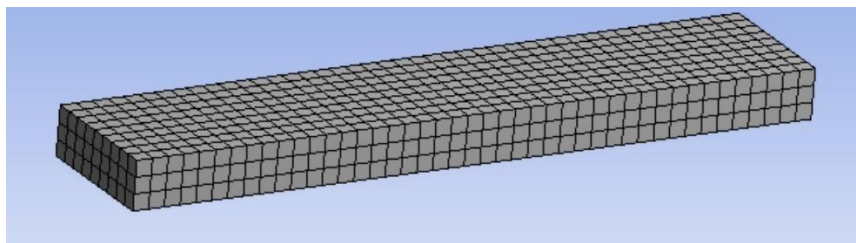


Fig. 6: 3 -D Straight channel model.

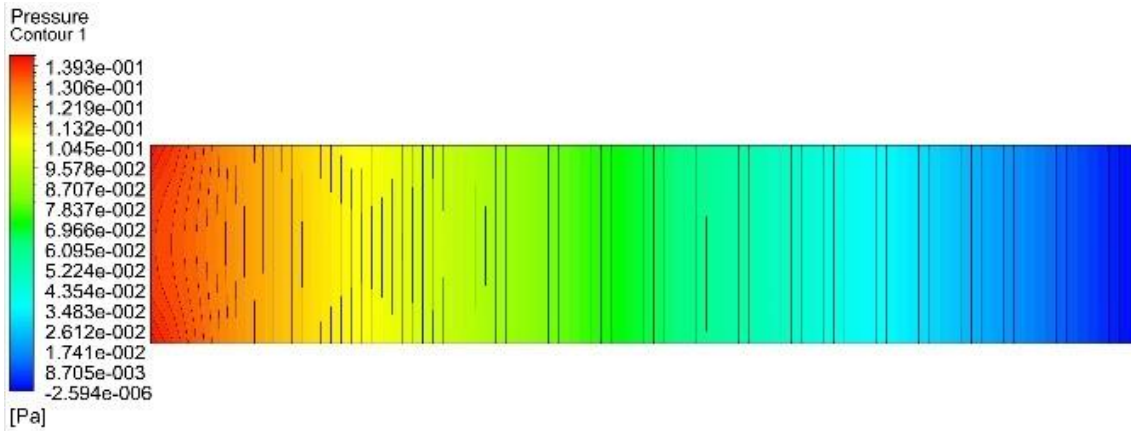


Fig. 7a: Numerical simulation results - Pressure distribution (Pa)

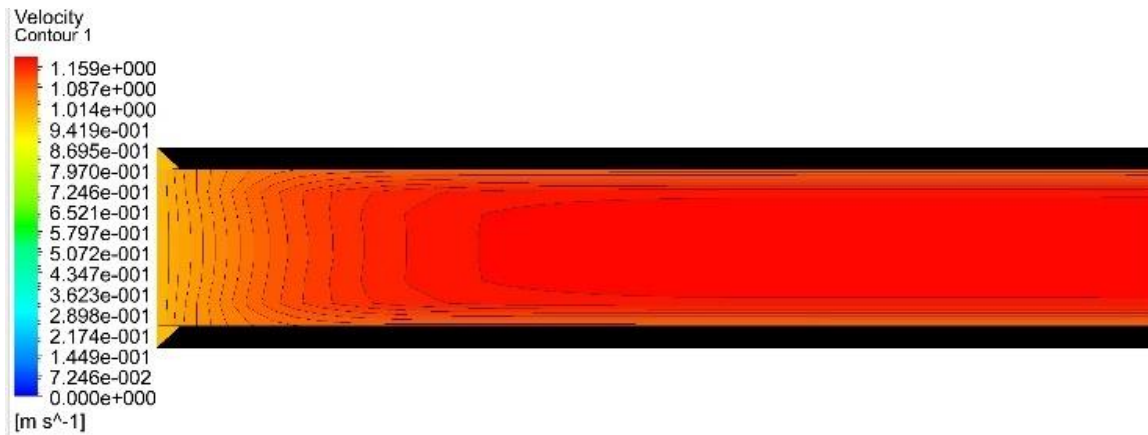


Fig. 7b: Numerical simulation results – Velocity (m/s)

From the simulation result, the pressure drop from the inlet to the outlet is fairly even with an increase in velocity of the gas from the inlet to the out.

Fig. 8 Shows a plot of the average pressure drop through this flow channel with some selected velocities (1, 3, 6, 9 and 12 m/s) already used in literature.

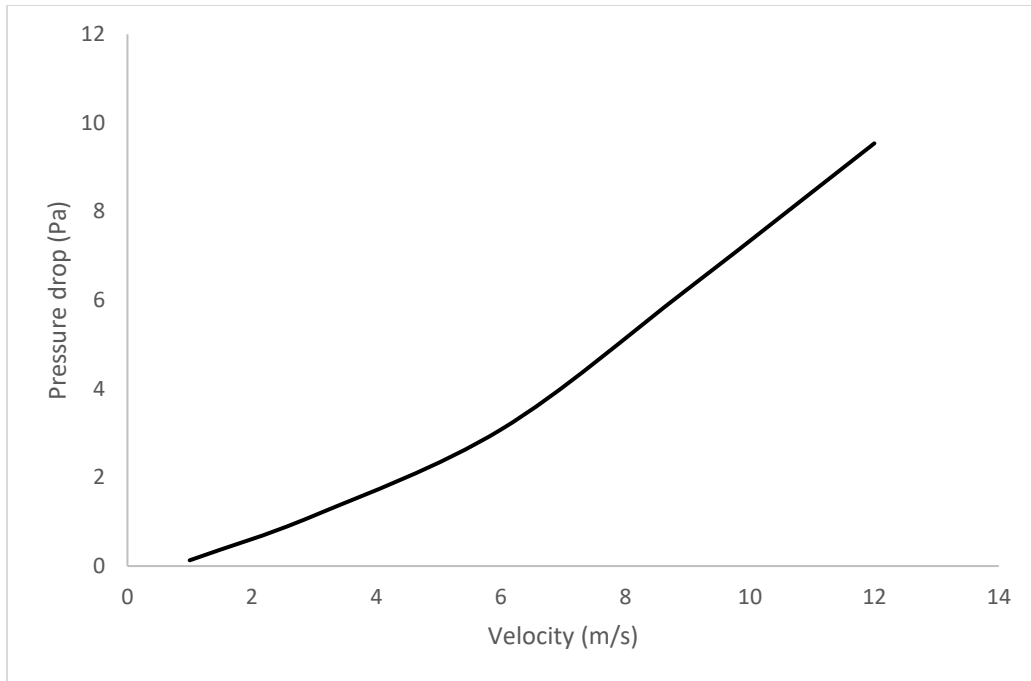


Fig. 8: Plot of Velocity against pressure drop through the representative channel

Mesh 2

The second mesh in the same manner but using tetrahedron elements and the patch conforming method. The size function was maintained at proximity and curvature and the relevance centre was maintained on the coarse setting. The transition setting was “slow”. These settings resulted in 2,156 nodes and 9391 elements.

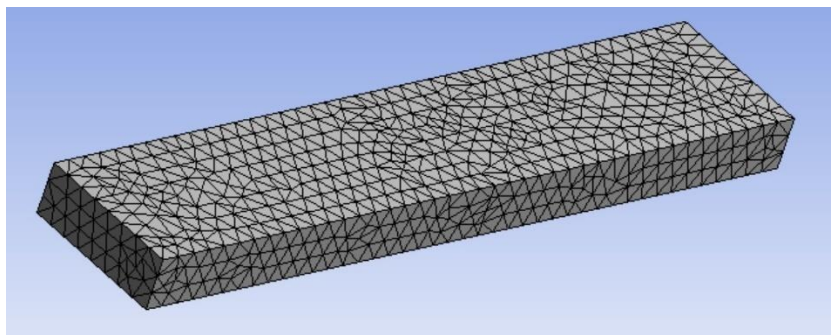


Fig. 9: 3-D Straight representative channel model for mesh 2

The velocity profile and pressure drop for mesh design 2 for the horizontal channel is shown in Figs. 10a and 10b. It can be seen that increasing the number of mesh elements resulted in a better resolution of the pressure drop contour as well as the velocity pressure contour. The pressure drop again is evenly distributed with the velocity profile showing signs of high velocity at the inlet and low velocity at the outlet. Fig. 11 also shows a plot of the average of the various selected velocities against the pressure drop.

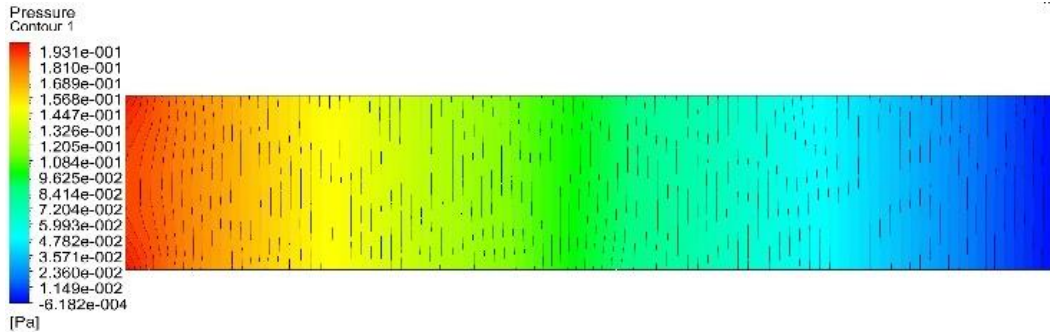


Fig.10a: Numerical simulation results - Pressure distribution (Pa)

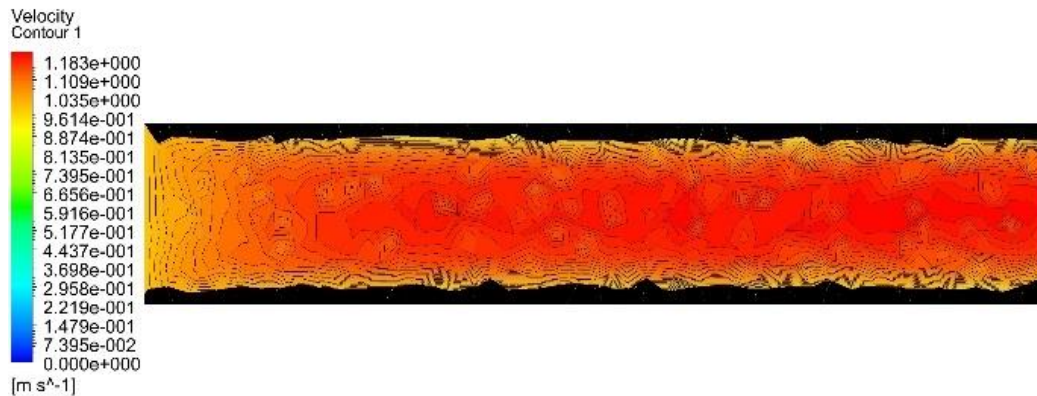


Fig. 10b: Numerical simulation results – Velocity (m/s)

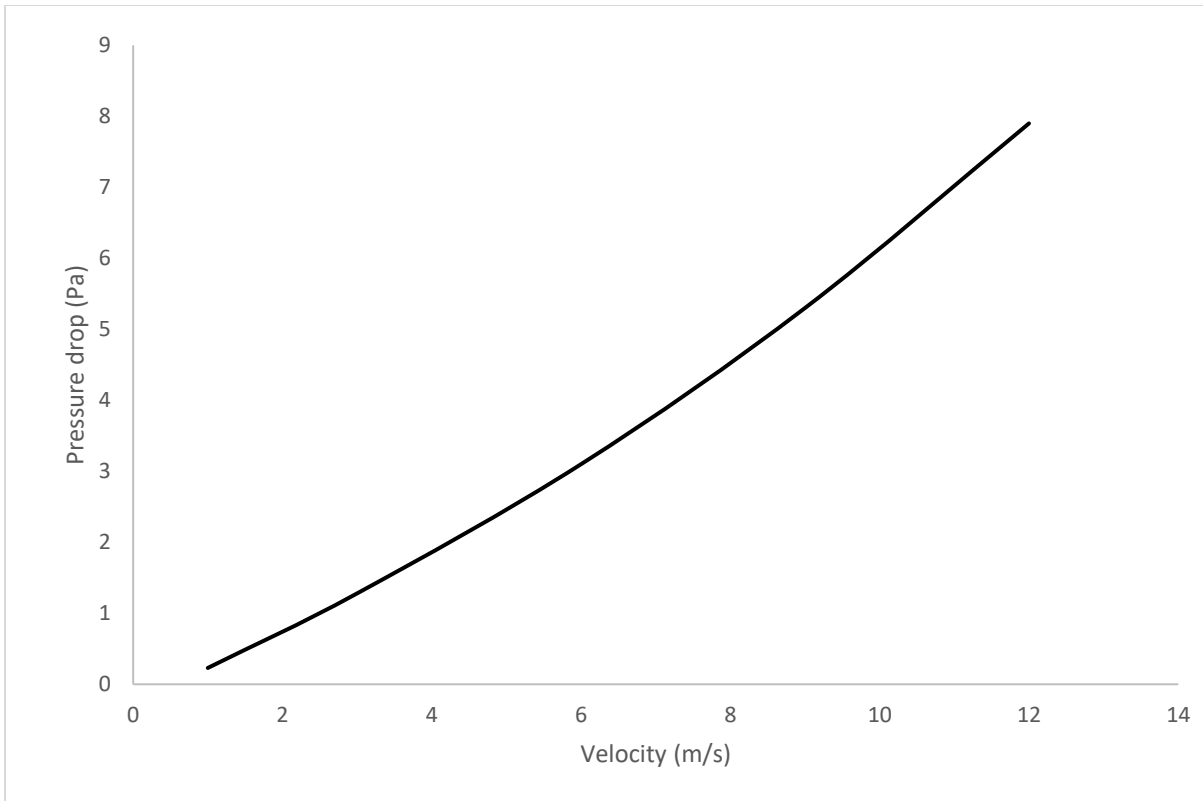


Fig. 11: Plot of Velocity against pressure drop through the representative channel

Mesh 3.

The same approach was followed for the geometry but the settings of the meshing engines were modified. Again tetrahedron elements were created using the patch conforming method as shown in Fig. 12.

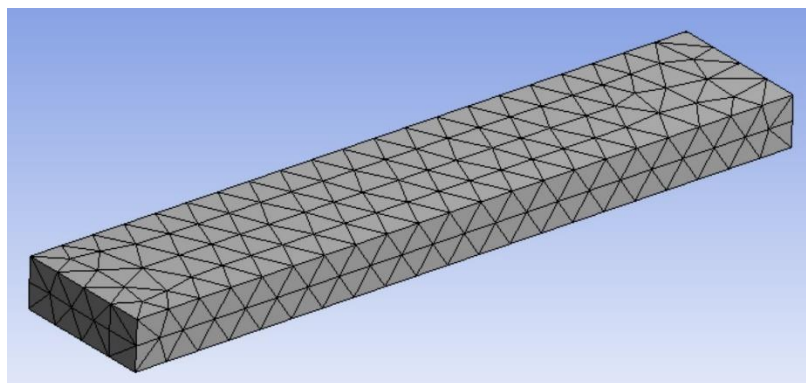


Fig. 12: 3 -D Straight representative channel model for mesh 3

Proximity and curvature were used for the size function, the relevance centre was kept on the coarse setting and the transition was kept on low. Figs. 13a and 13b show the velocity profile and pressure drop through the representative geometry. Fig. 14 shows the plot of the velocity of the fluid against the pressure drop. This mesh gives very low values for the pressure. +

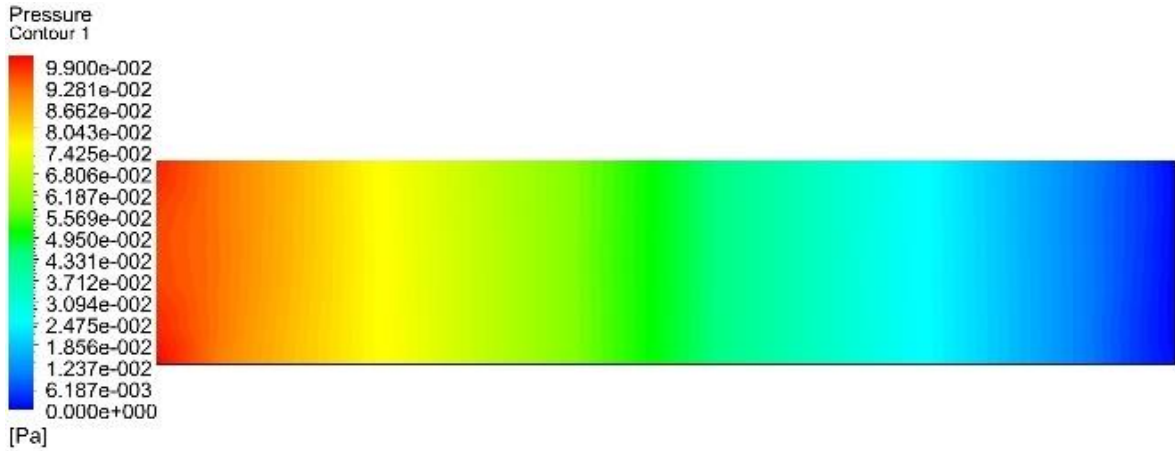


Fig. 13a: Numerical simulation results - Pressure distribution (Pa)

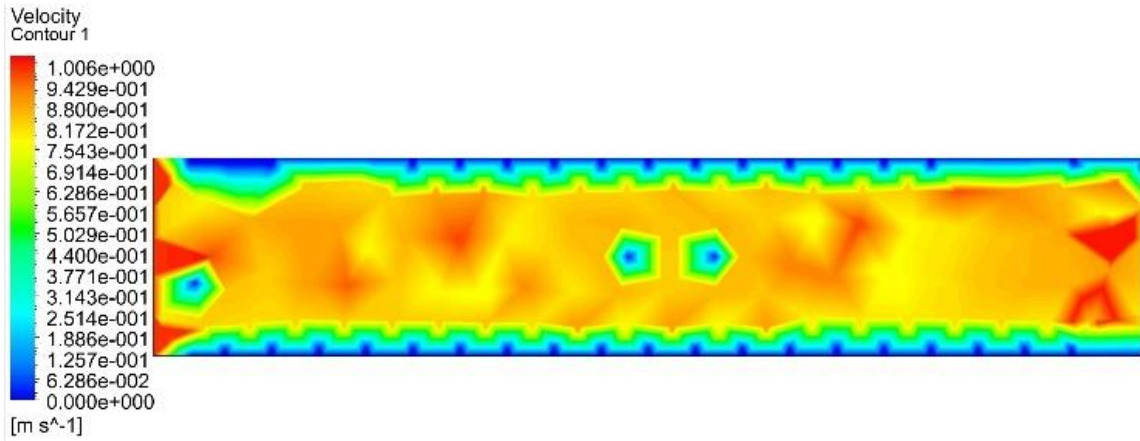


Fig. 13b: Numerical simulation results - Velocity(m/s)

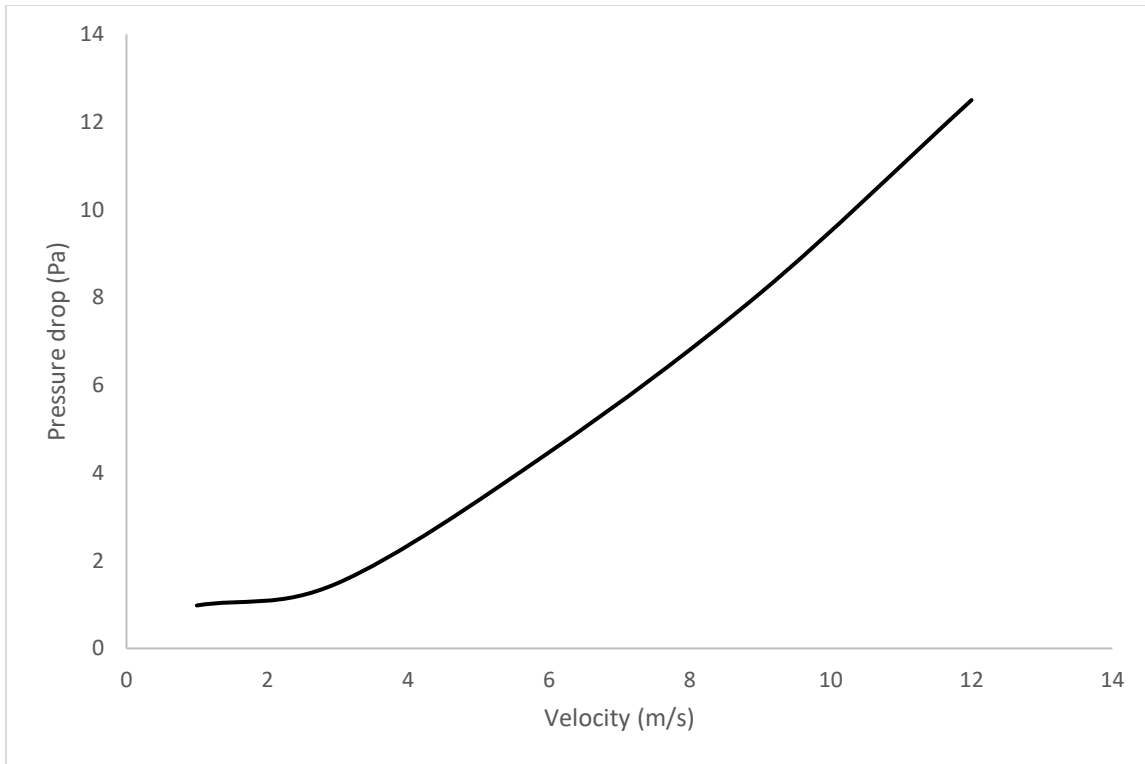


Fig. 14: Plot of Velocity against pressure drop through the representative channel.

Mesh 4

The fourth mesh was created used most of the previous setting with the relevance centre set to “fine”. The transition was set to “slow”. This resulted in 20,816 nodes and 106,883 elements as depicted in Fig. 15.

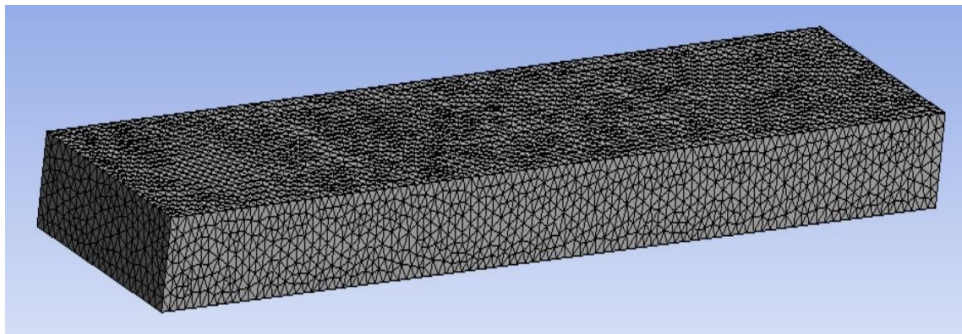


Fig. 15: 3 -D Straight channel model for mesh 4

A much better resolution was obtained for both the pressure and the velocity fields than in the previous three attempts. Results are shown in Figs. 16a, 16b and 17.

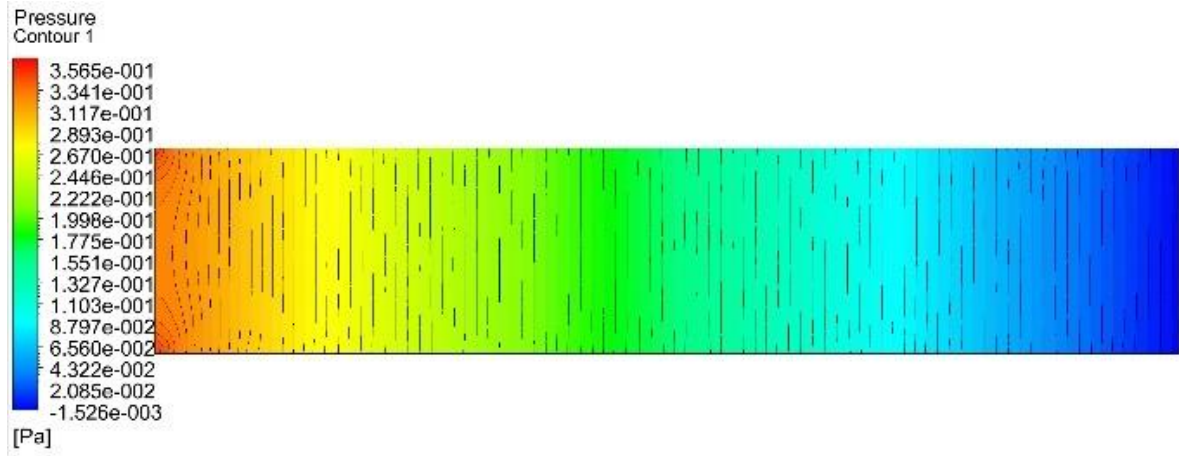


Fig. 16a: Numerical simulation results - Pressure distribution (Pa)

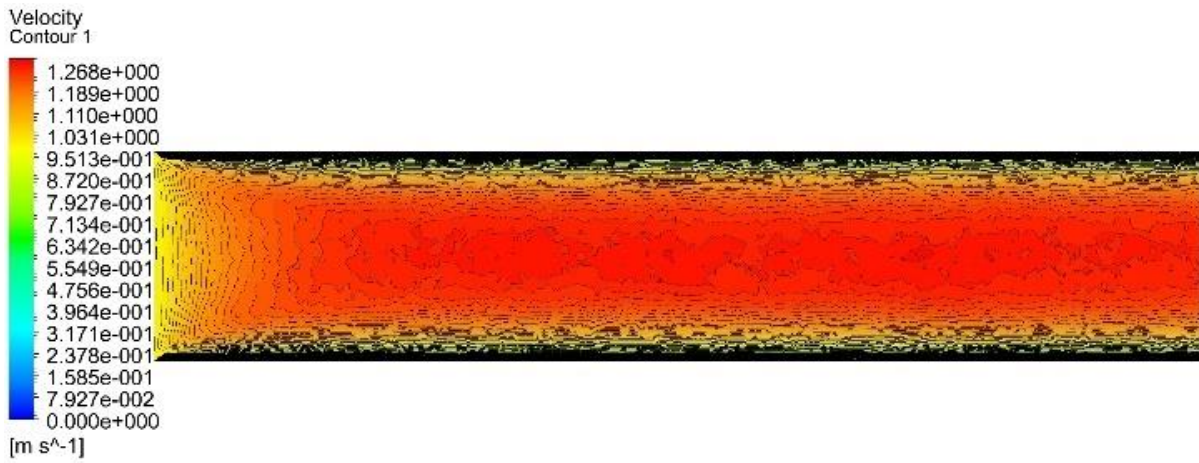


Fig. 16b: Numerical simulation results - Velocity (m/s)

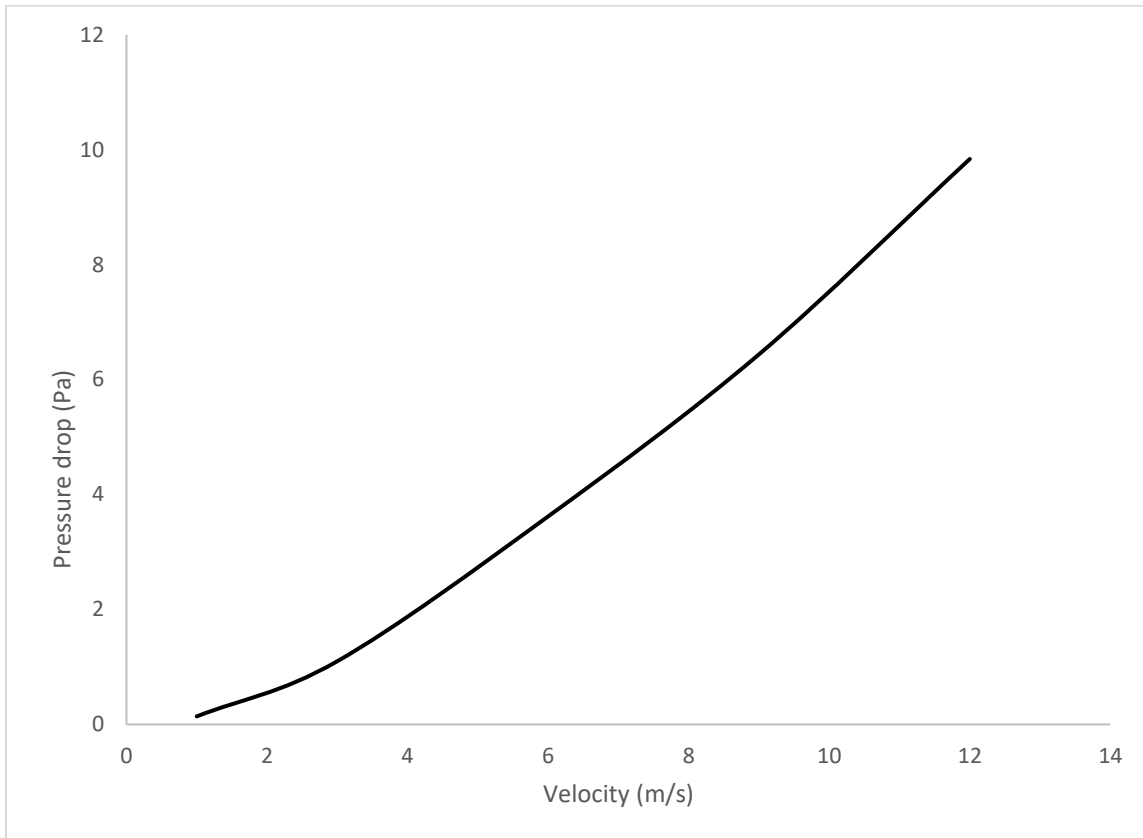


Fig. 17: Plot of Velocity against pressure drop through the channel.

Fig. 18 is a comparison between the various mesh designs considered through the simulation process and hence a conclusion was drawn that maintaining the element as high as possible was going to give an idea of the pressure drop that would occur for each of these elements as the fluid flows through the domain.

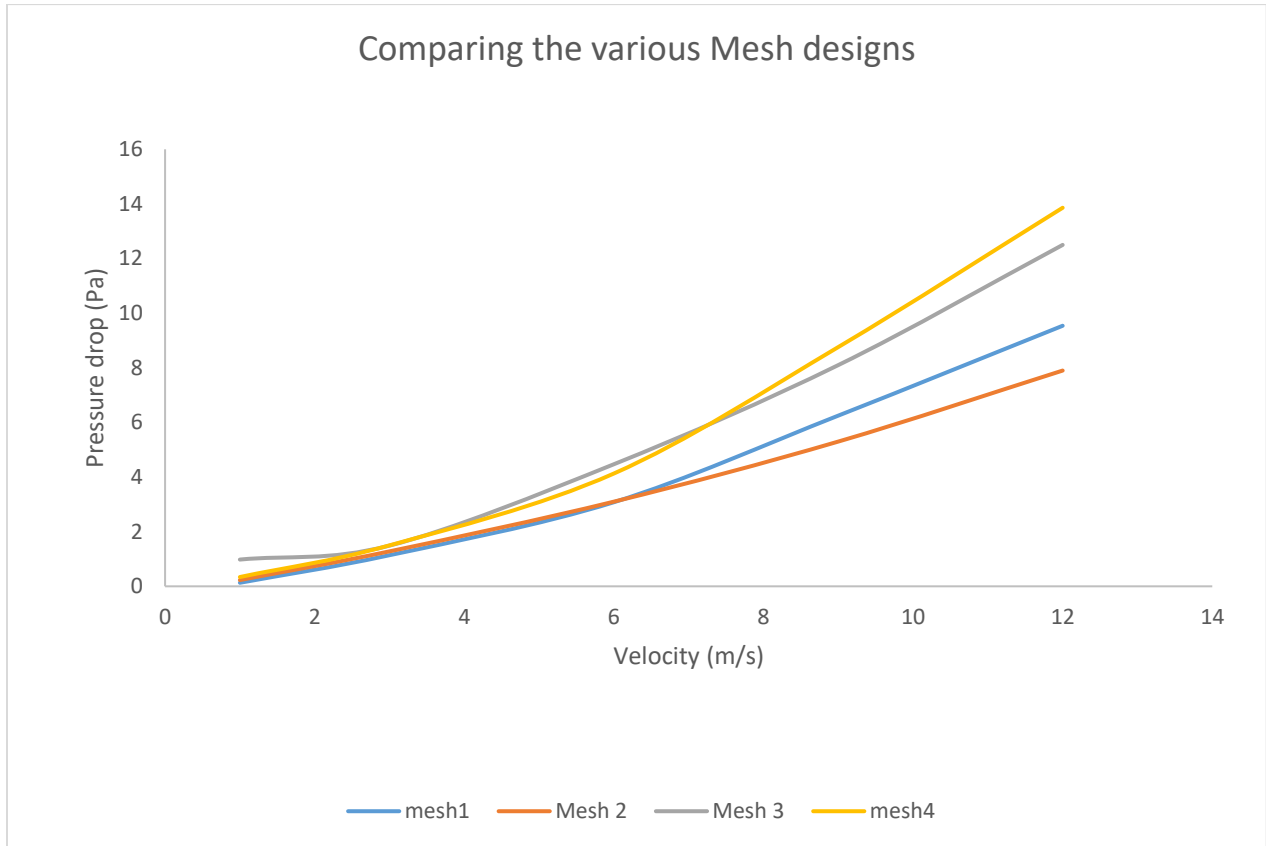


Fig. 18: A plot comparing the various mesh designs considered during the simulation process.

Once the mesh was carefully studied and validated, the rest of the modifications to be made on the existing flow plates were simulated in CFD with a finely divided grid. This helps improve the resolution and gives a better prediction of the pressure drop that occurs through the selected fluid domain.

The next stage of the simulation process was to run some simulations for the flow plate designs used in the making of fuel cells on the market and those covered in the literature. This was to give an idea of the likely pressure drop through these flow plates. Once these values were determined, another simulation process was conducted but this time with the modified designs. Finally, both designs were compared with each other and the best option was selected.

Serpentine flow plate

The serpentine flow plate design in fuel cells has been investigated by several researchers around the world [20] and it is considered as the standard for flow design in most fuel cells. Several companies use this design as their main flow plate design in manufacturing of PEM fuel cells because it supports the full usage of the active area and coverage of gas at reasonable pressure losses. Fig. 19 shows a typical design of a serpentine flow plate used in fuel cells.

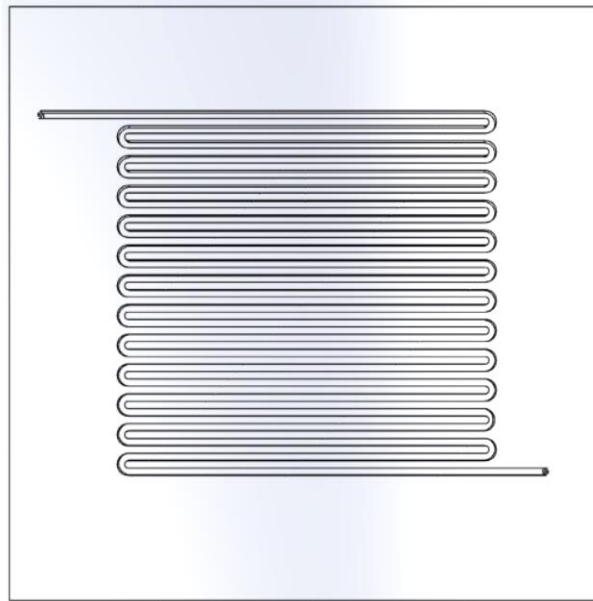


Fig 19: Typical Serpentine Flow Plate Design in a Fuel Cell.

The double serpentine channelled flow plate with ribs and channels 1mm wide and 1mm deep as shown in Fig.19 is the most commonly used configuration. This flow plate design was first modelled in solid works then analysed using ANSYS CFD (CFX) to develop proper understanding of its operation and gain the necessary knowledge for subsequent design modifications.

The simulations were done to develop an understanding of fluid flow in the plates and the results obtained corresponded with what existed in literature such as the works of Carton et al [1]. The main design issues were identified and this knowledge contributed to the modified design of the new serpentine fluid flow plates. Table 4 shows the simulation parameters and the properties used.

Table 4. Simulation parameters used throughout the entire simulation

Modeller	ANSYS DM
Mesher	ANSYS Meshing
Mesh	Mixed Tet and Quad
Sizing	Proximity and Curvature
Smoothing	Coarse
Transition	Slow
Elements	316,853
Solver	CFX
Model flow	Laminar
Fluid	Hydrogen
Solid walls	Aluminium
Porosity	0.90
Inlet Velocity	10m/s
Temperature	288
Porous GDL	0.90
Monitors	Mass flow Continuity
Interfacial area density	0.50
Heat transfer coefficient	0.01
Iteration	100
Solver type	Pressure based – Double precision

Serpentine Design Simulation

As explained earlier, this design supports the flow of the gas through almost all the entire surface of the MEA. From the simulation results in Fig. 20a, it is observed that there is high inlet pressure on the first inlet channels. This pressure gradually drops from the inlet to the outlet, a clear indication that the pressure within the MEA decreases from inlet to the outlet as expected. The mass transport and the general performance of the fuel cell are governed by these

characteristics of the PEM fuel cell. Fig. 20a shows that there is an even distribution of the velocity field of the fluid (hydrogen and air) throughout the entire flow plate and the flow covers the full area of the MEA being supplied with the gas (hydrogen or air). The serpentine flow plate design ensures a constant flow of the fluid through the channels and this in effect helps remove any excess liquid that may condense in the fuel cell such as water that may block the channels by transporting it to the outlet easily. A boundary layer is observed at the channel walls with water often accumulating near the wall creating annular gas flow. The blue region on the pressure simulation shown in Fig. 20b indicates a region of possible dead zones. This indicates areas within the channel where the gas might not be in contact with the membrane and this indicates the need for modification of this design.

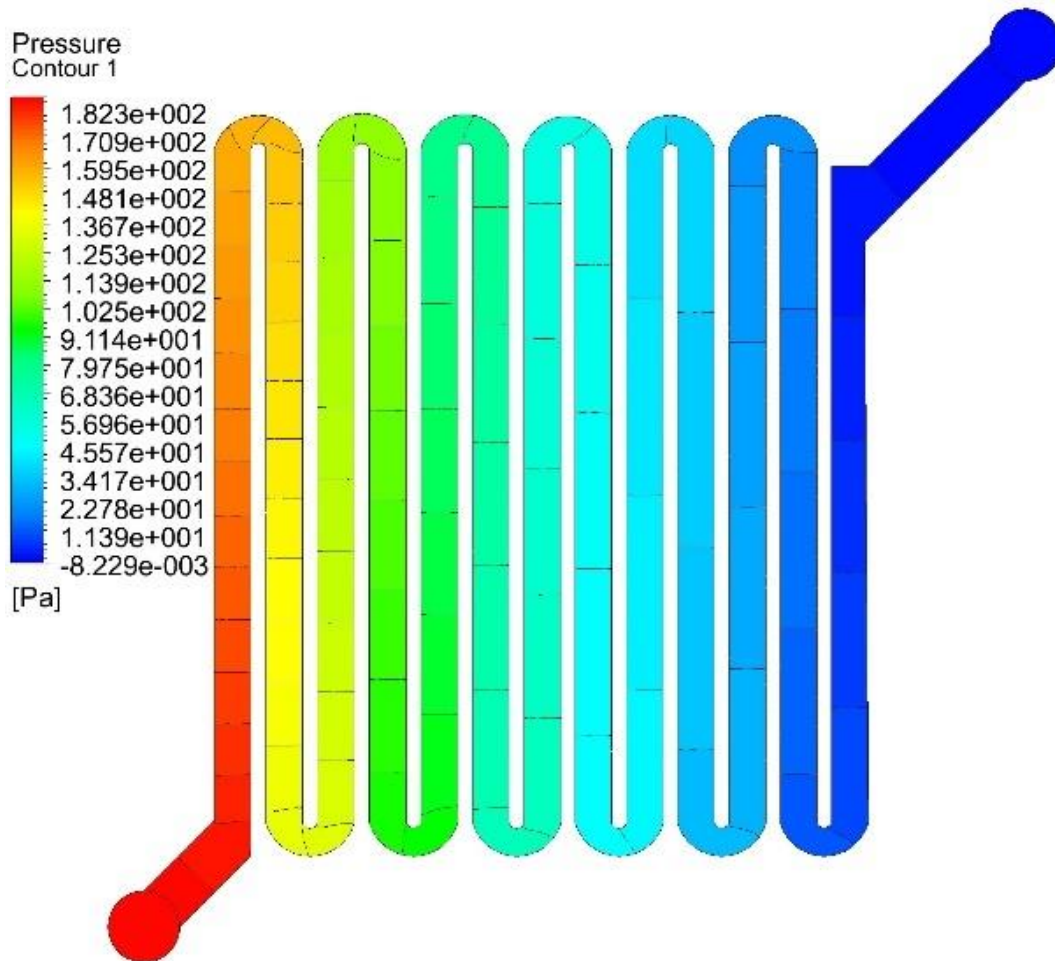


Fig. 20a: Numerical simulation results of Serpentine flow plate - Pressure distribution (Pa)

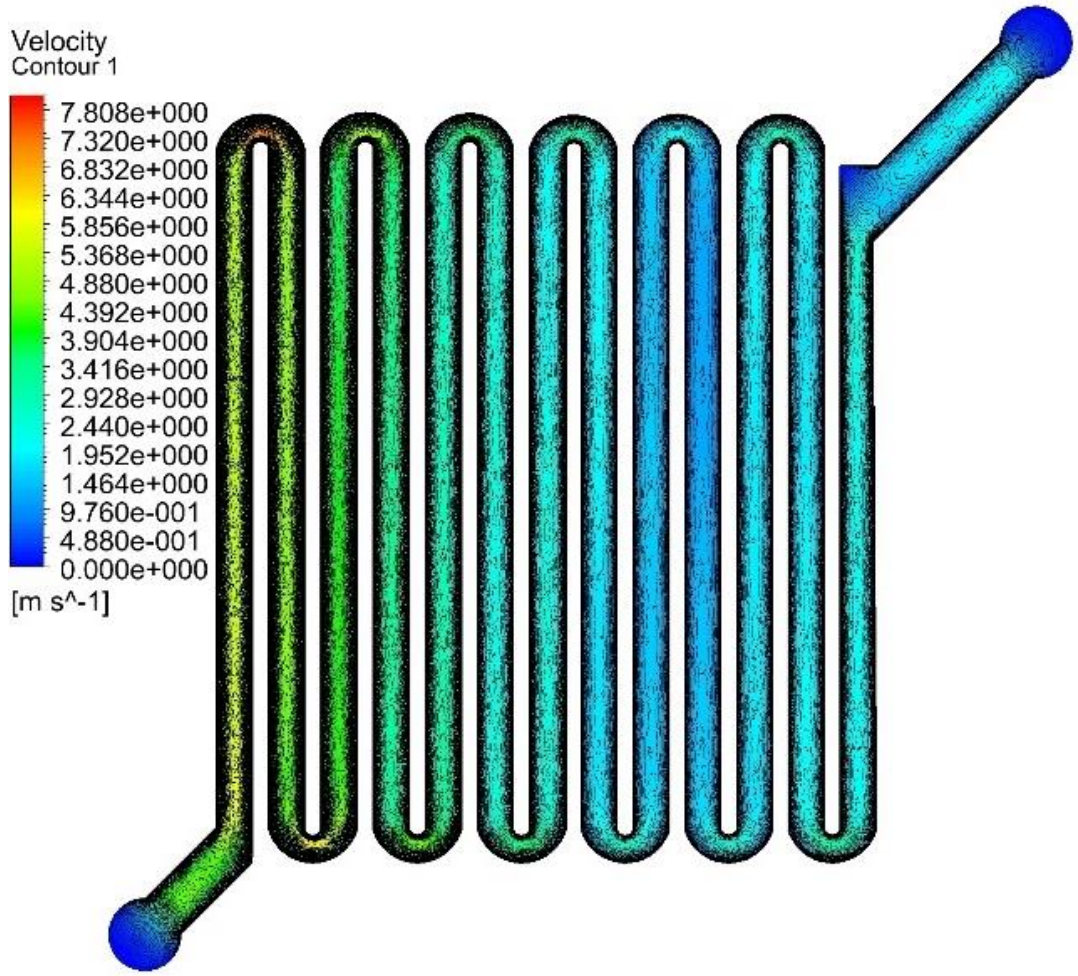


Fig.20b: Numerical simulation results of Serpentine flow plate - Velocity vectors (m/s)

Parallel flow plate design

Another design that is considered as a standard and used in the industry is the parallel flow plate. Simulation was performed on this design with some key parameters carefully analysed during the simulation process. The removal of water and an even distribution of the gas throughout the plate flow area to fully utilise the gas diffusion layer (GDL) were carefully considered. The design should be able to improve pressure distribution throughout the flow plate because all the channels would have equal access to the input gas channel as shown in Fig. 21.

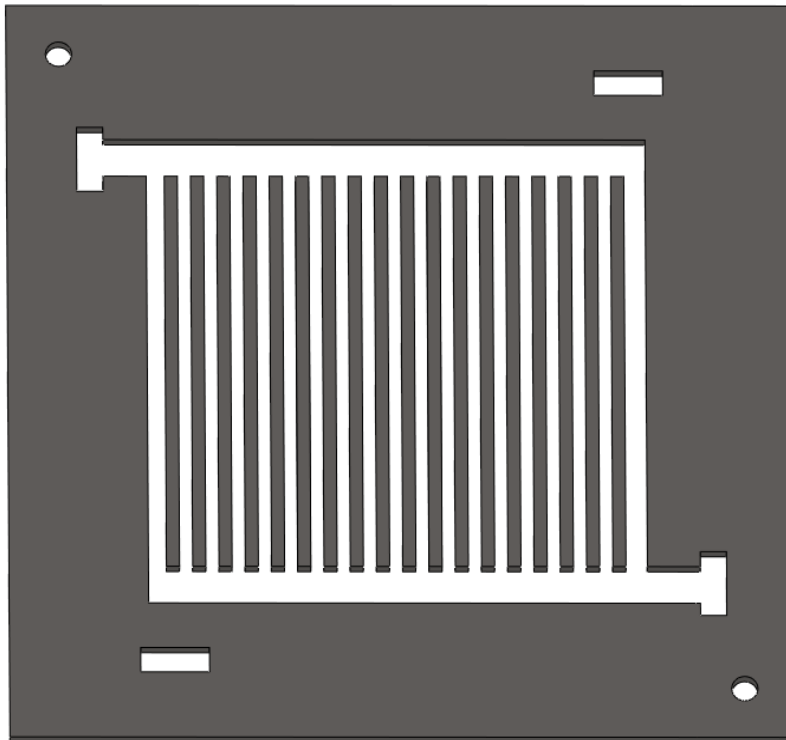


Fig. 21: Parallel flow plate design

The design aims to improve the pressure distribution throughout the plate flow area because all the channels (1mm wide and deep) would have the same access to the input gas.

The pressure distribution as shown Fig. 22a indicates high pressures in the inlet region, low pressures at the outlet region as expected. Channels nearer to the dead end of the inlet zone develop high pressure drops compared with those further away. This was a major driver for the modification which will be shown later.

On the other hand, Fig. 22b shows an even velocity distribution throughout the plate flow region indicating that the differences observed in the pressure contour are not strong enough to affect the flow in the channels appreciably.

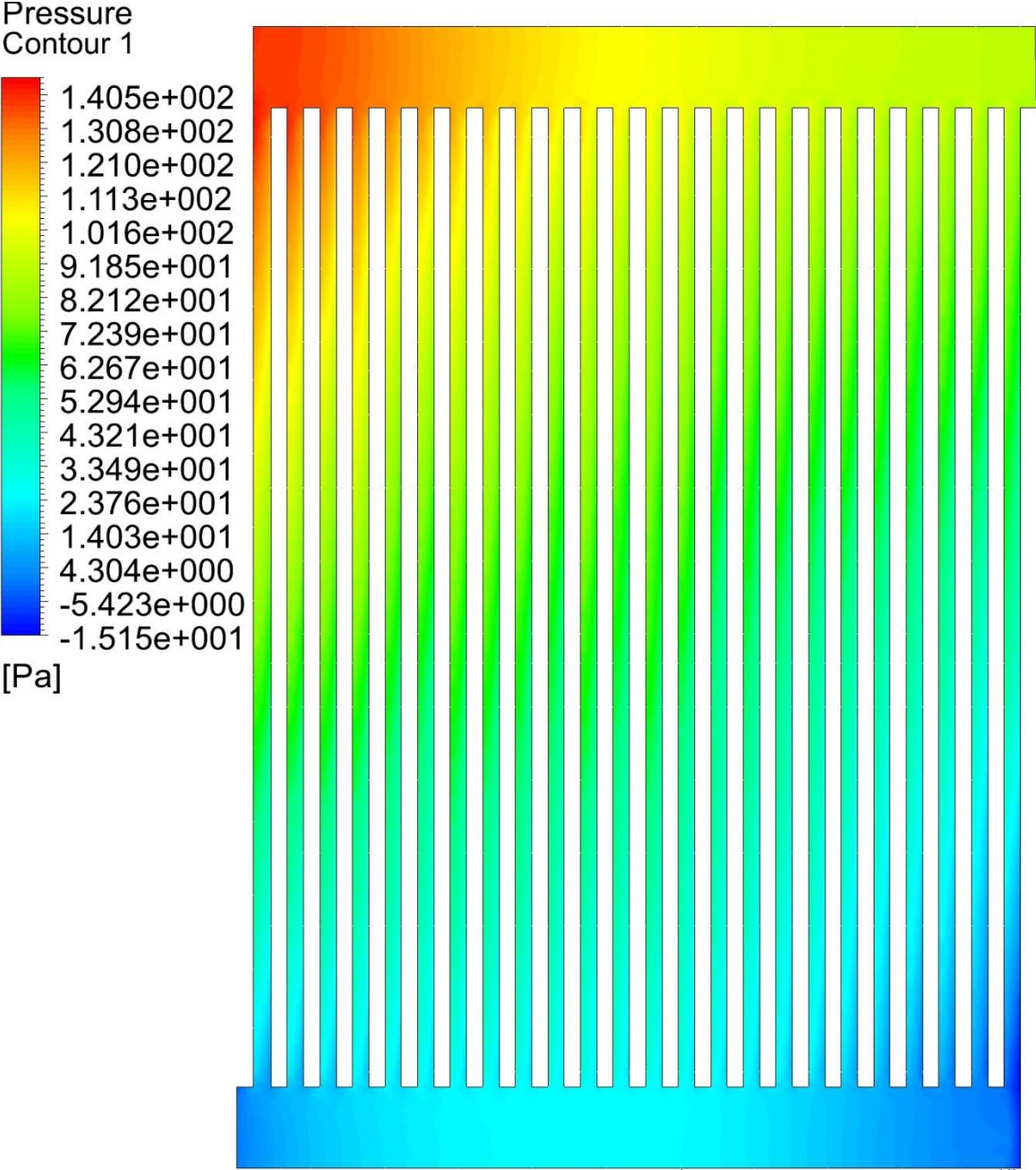


Fig.22a: Numerical Simulation Results of Parallel Flow Plates - Pressure distribution (Pa)

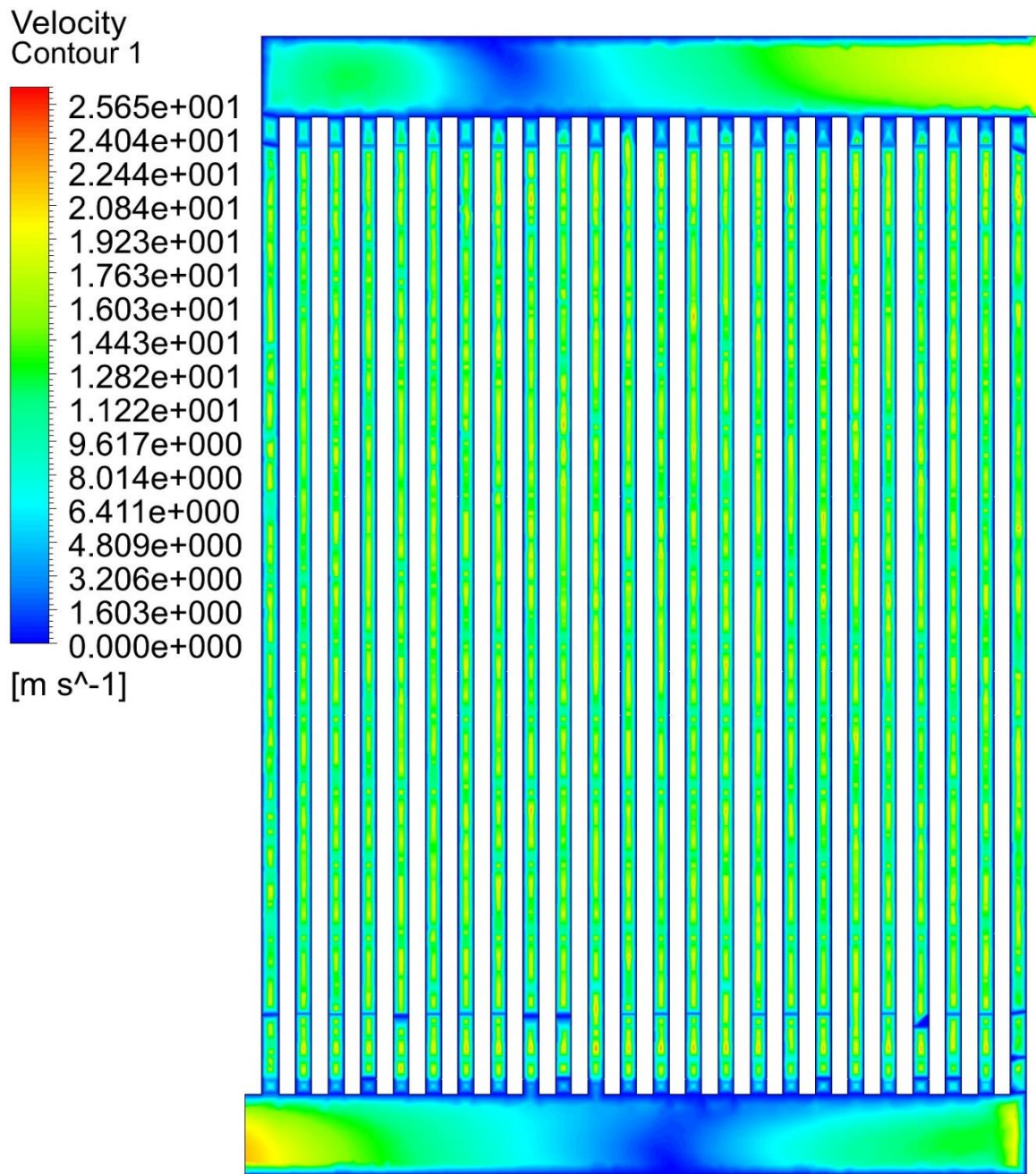


Fig.22b: Numerical Simulation Results of Parallel Flow Plates - Velocity (m/s)

Pin Flow Plate Design

The Pin flow plate design in literature was modified using the same injector design. The common design of the Pin flow in literature has 2 mm pin embedded in the plate. The purpose of these pins is to help in the distribution of the fluid uniformly through the flow plate and also ensure large contact area with the MEA.

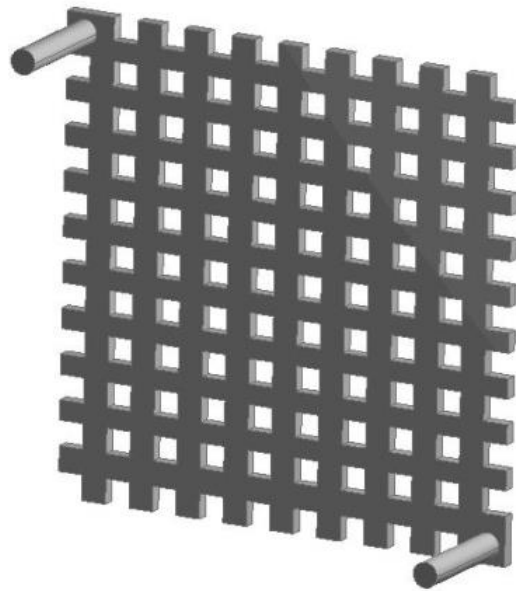


Figure 23: Pin flow plate design

The pressure distribution through the pin flow plate shown in Fig. 24a indicates a lower pressure drop with a plate gauge pressure of 16 Pa on the inlet side and a gauge pressure of 3 Pa on the outlet side. However, the velocity profile, Fig. 24b shows a velocity of 1.7m/s at the plate inlet side which is low compared to other designs.

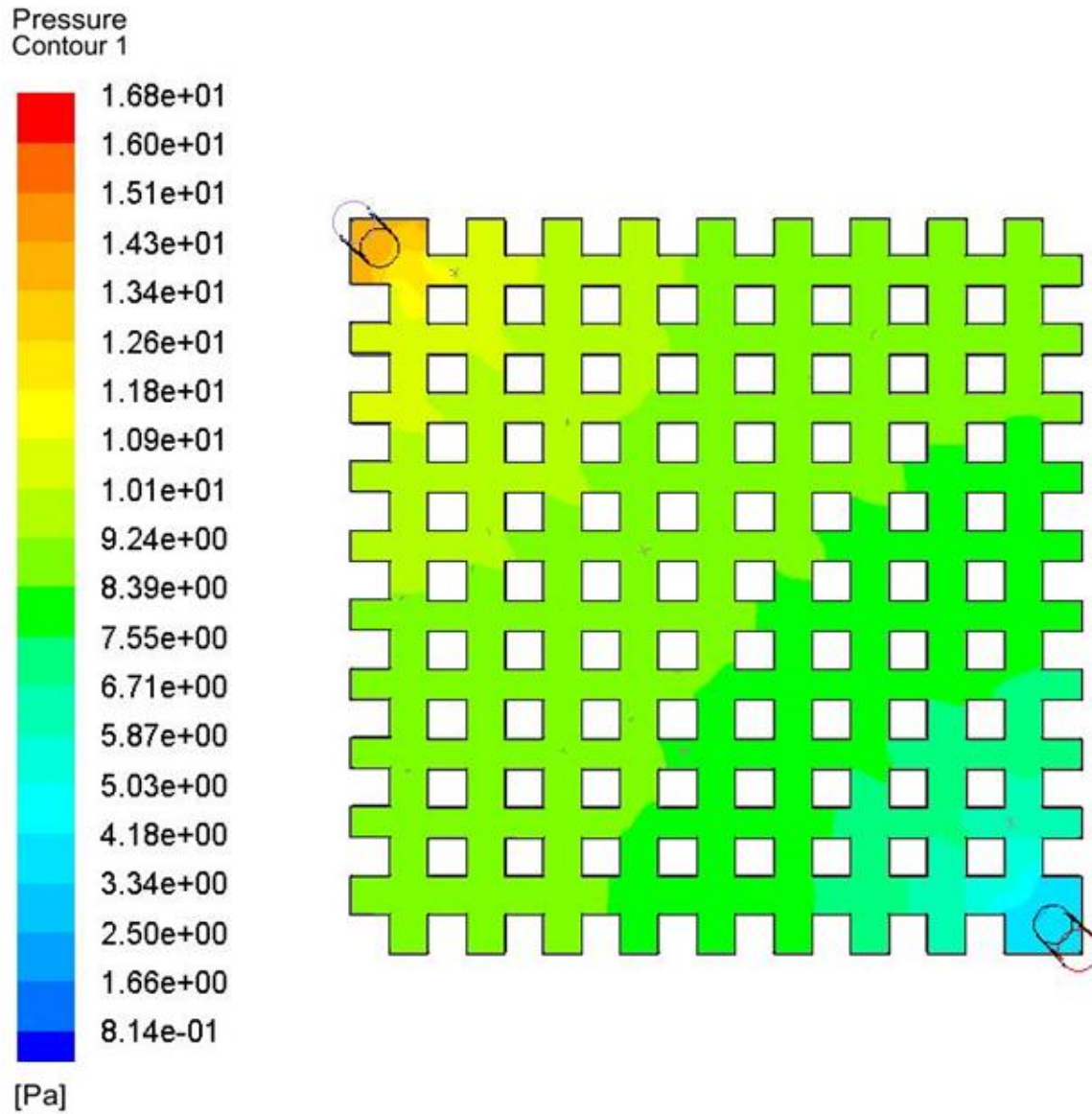


Fig.24a: Numerical simulation results of Pin flow plates - Pressure distribution (Pa)

Velocity
Contour 1

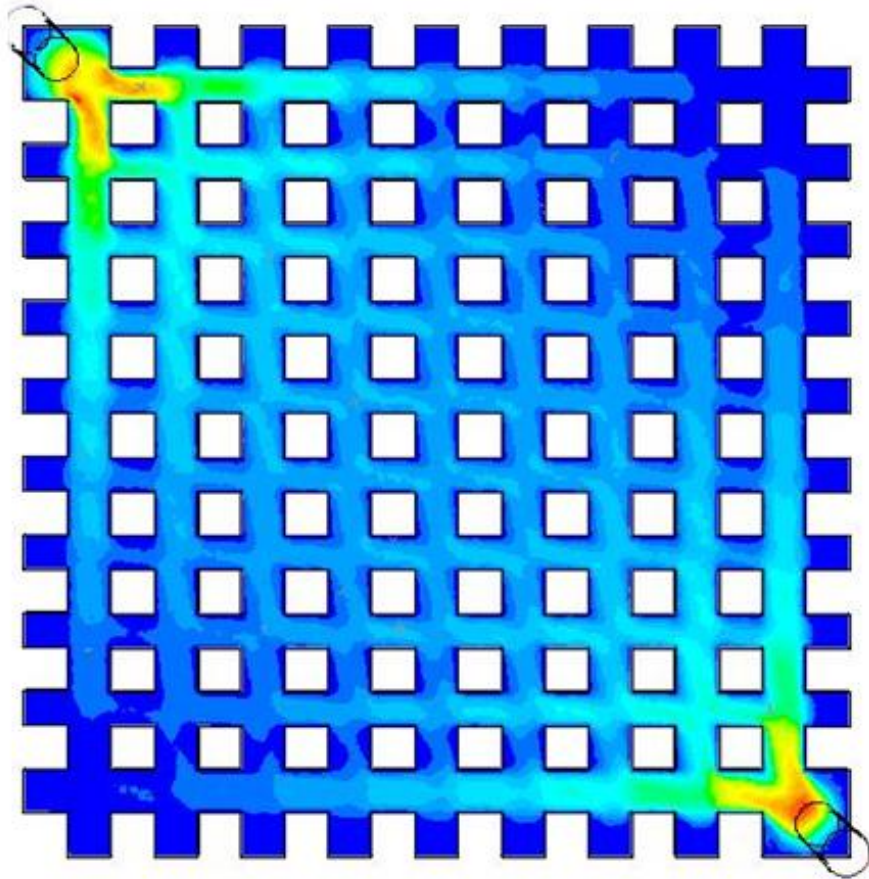
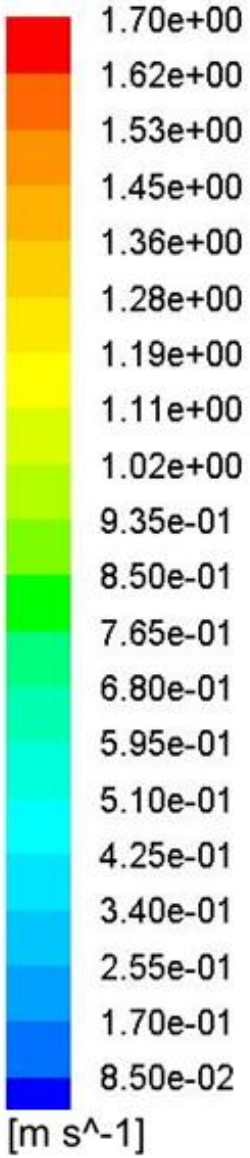


Fig.24b: Numerical simulation results of Pin flow plates - Velocity (m/s)

Interdigitated flow plate design

The interdigitated flow plate is one of the designs in the literature [3] which has not yet been explored by researchers to a larger extent. The design is often a dead end with several ribs and channels. It implies that the gases are forced through the GDL when it enters the inlet flow field. It then leaves the GDL exits the flow plate.

Fig 25 shows a diagram of interdigitated flow field design. The plate is expected to develop high pressure drop due to the large separation losses at the end of the individual channels.

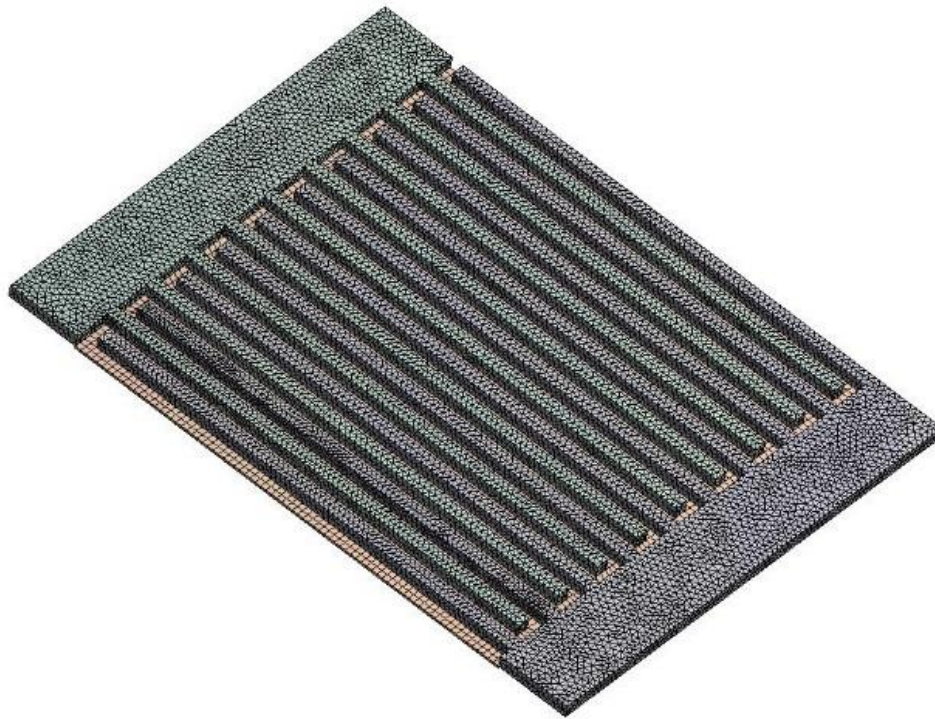


Fig. 25: Interdigitated flow field design.

Modified design for serpentine flow plate with 2 bypass channels

This design was modelled out of the serpentine design described in the literature. The inlet of the design is some few millimetres away from a gap that leads to the mid region of the flow plate where the MEA is found. The left and right side of the design have bypass channels where the gas can travel through to the outlet. The mesh was generated using tetrahedron elements with the patch conforming algorithm.. A fine mesh was produced with 200,764 nodes and 938590 elements as shown in Fig. 26.

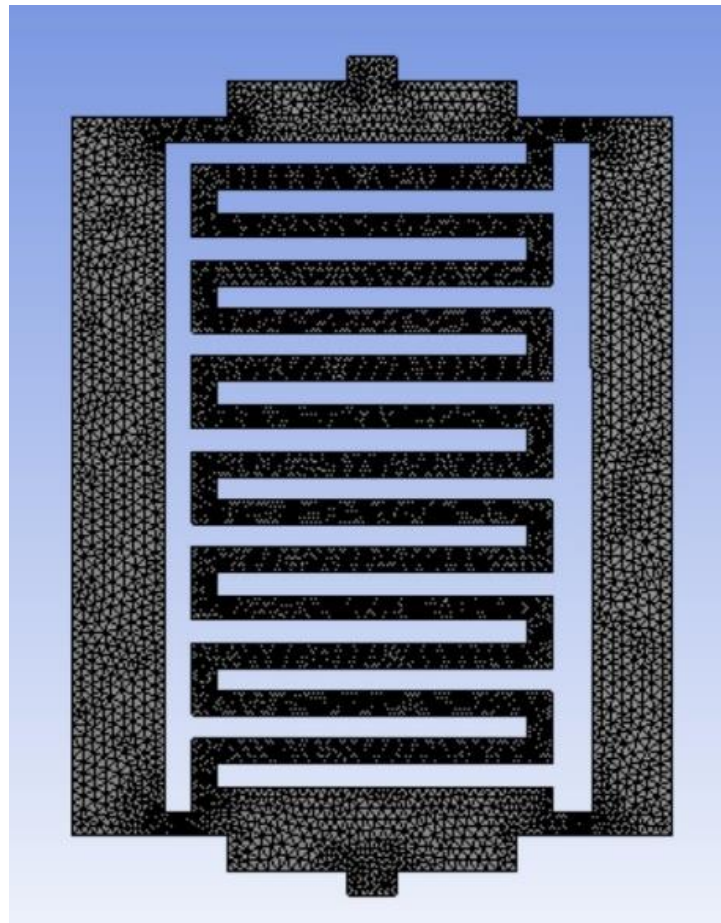


Fig. 26: Meshing of modified serpentine flow plate design

Fig. 27a shows the pressure contours for the modified design. Increasing the gap at the inlet will increase the amount of gas flowing at the mid region.

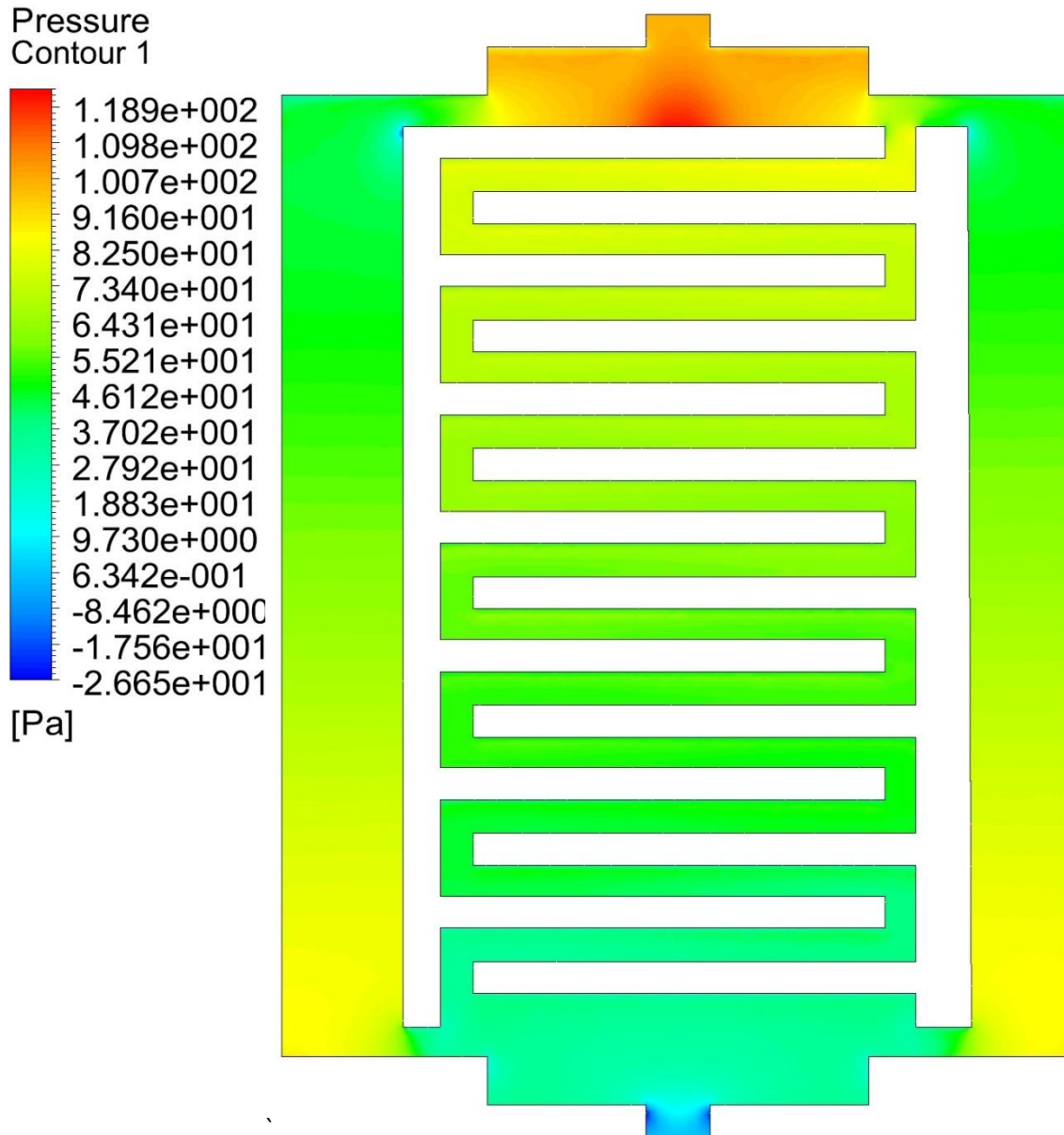


Fig. 27a: Numerical simulation results of the modified Serpentine flow design with 2 by pass channels - Pressure distribution (Pa)

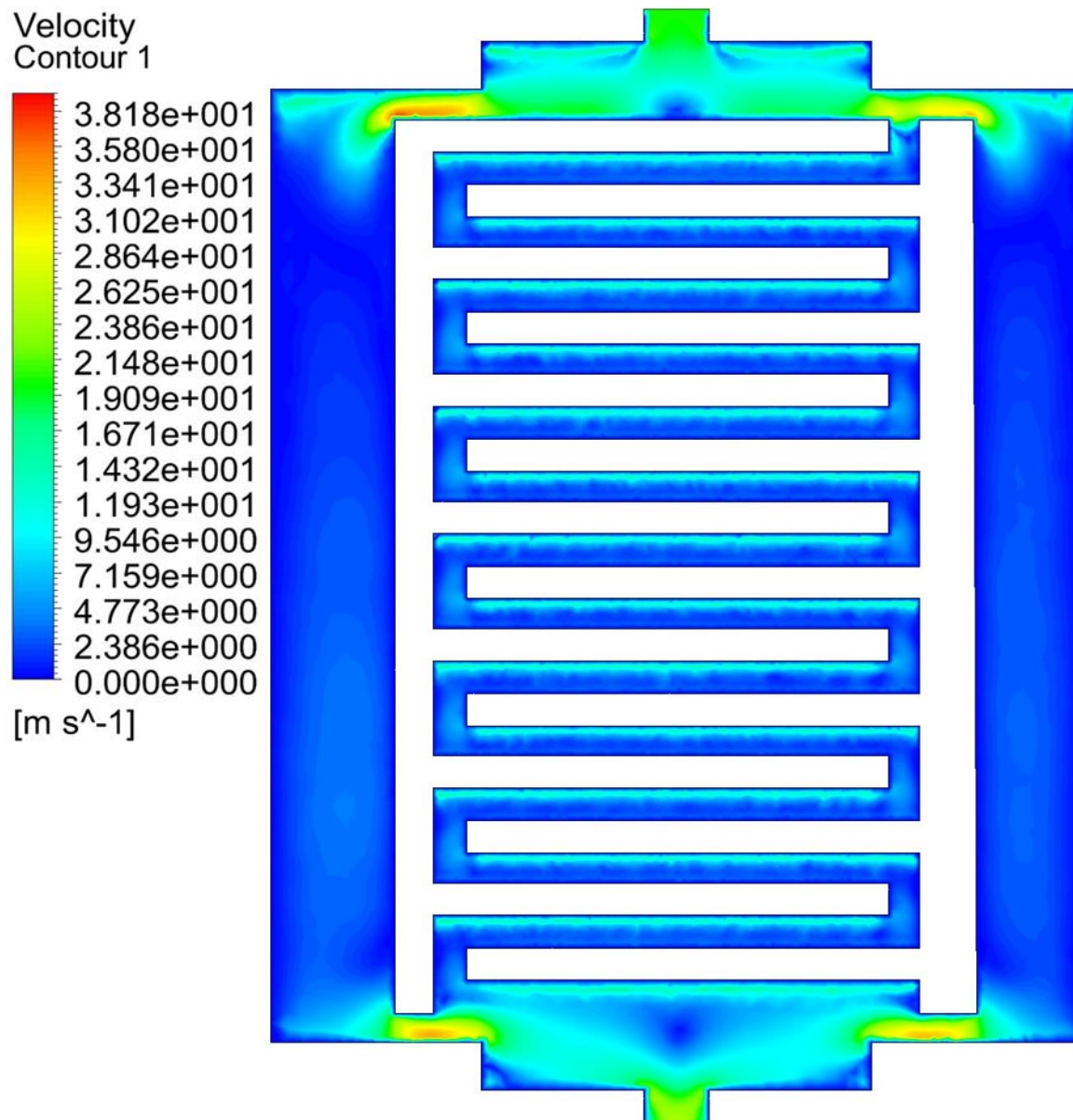


Fig. 27b: Numerical simulation results of the modified Serpentine flow design with 2 by pass channels- Velocity (m/s)

Fig. 27b shows the velocity contours in the modified cell. From the simulation results it is clear that appreciable gauge pressure develops to enable the gases to move through the channels to the discharge point which is at atmospheric pressure as shown in Fig 27a. The velocity of the gas flowing through the channels is slightly lower than the velocity in the original design due to

enlarged channel width (Fig. 27b). This will be of benefit as it increases the reactants residence time in the cell leading to higher conversion rates.

Modified Serpentine flow plate design with 4 bypass channels

It has been stated earlier that serpentine flow plates have large pressure drops but better performance characteristics than that of the parallel flow plate designs which operate with lower pressure drops. This design is therefore a combination of both the serpentine and the parallel flow channels to achieve a better performance resulting from the presence of the serpentine channel portion and at the same time ensure overall lower pressure drop due to the parallel bypass channels.

From Fig. 28a, the inlet gauge pressure of the modified serpentine with 4 bypass channel is 34 Pa with a total pressure drop of 32 Pa. There is consistent and even pressure drop from the inlet to the outlet and this design will equally help in water management. Existence of bypass channels ensures that for a series connection, blockage in the serpentine channel length will not hinder the flow through the other series connected flow plate in the fuel cell. Also, the possibility of dead zones or water accumulation is reduced due to the nature of the design. Water can easily flow through the channel from the inlet to the outlet reducing the possibility of flooding hence improving the water management of the cell.

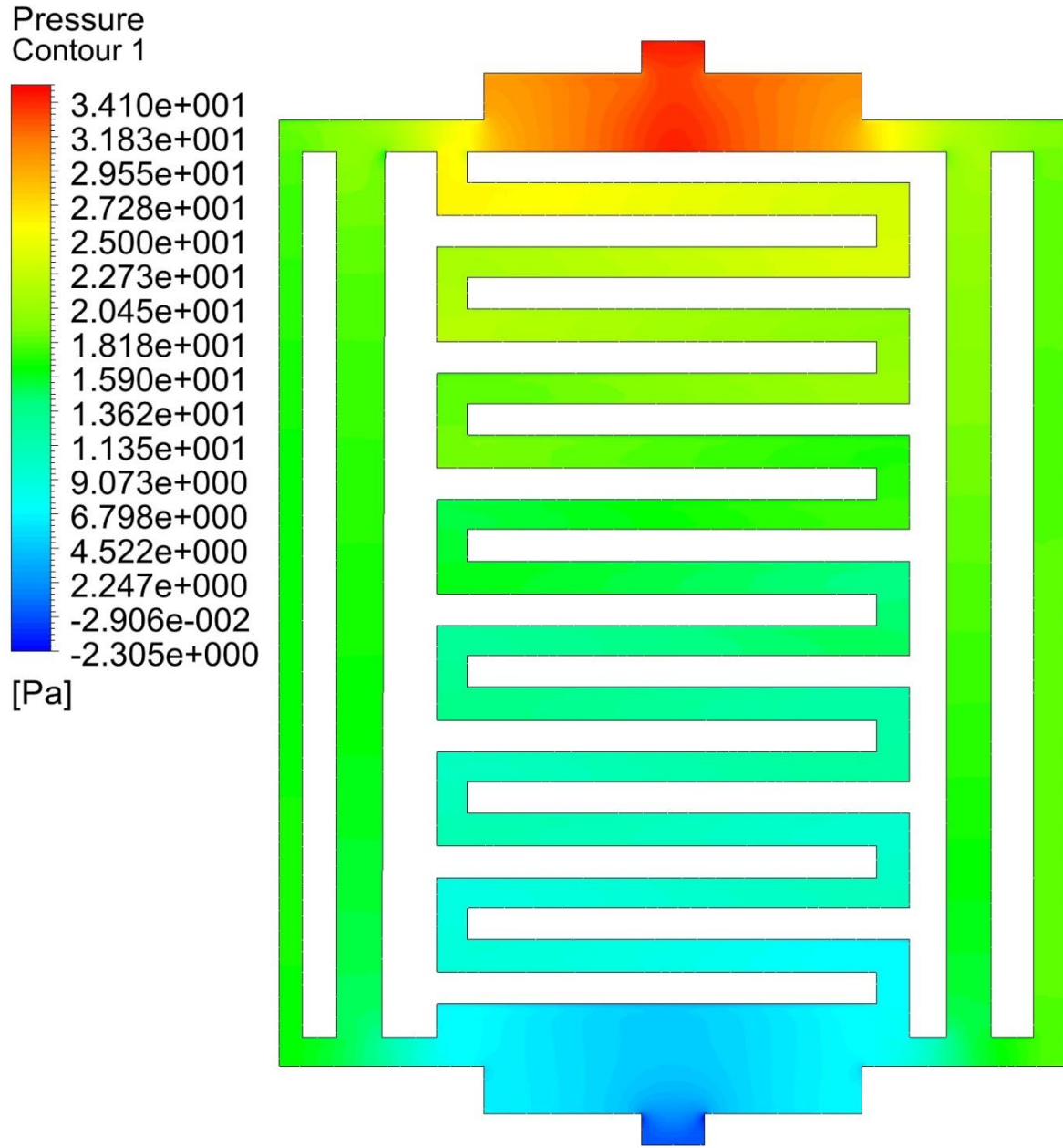


Fig. 28a: Numerical simulation results of the modified Serpentine flow design with 4 by pass channels - Pressure distribution (Pa)

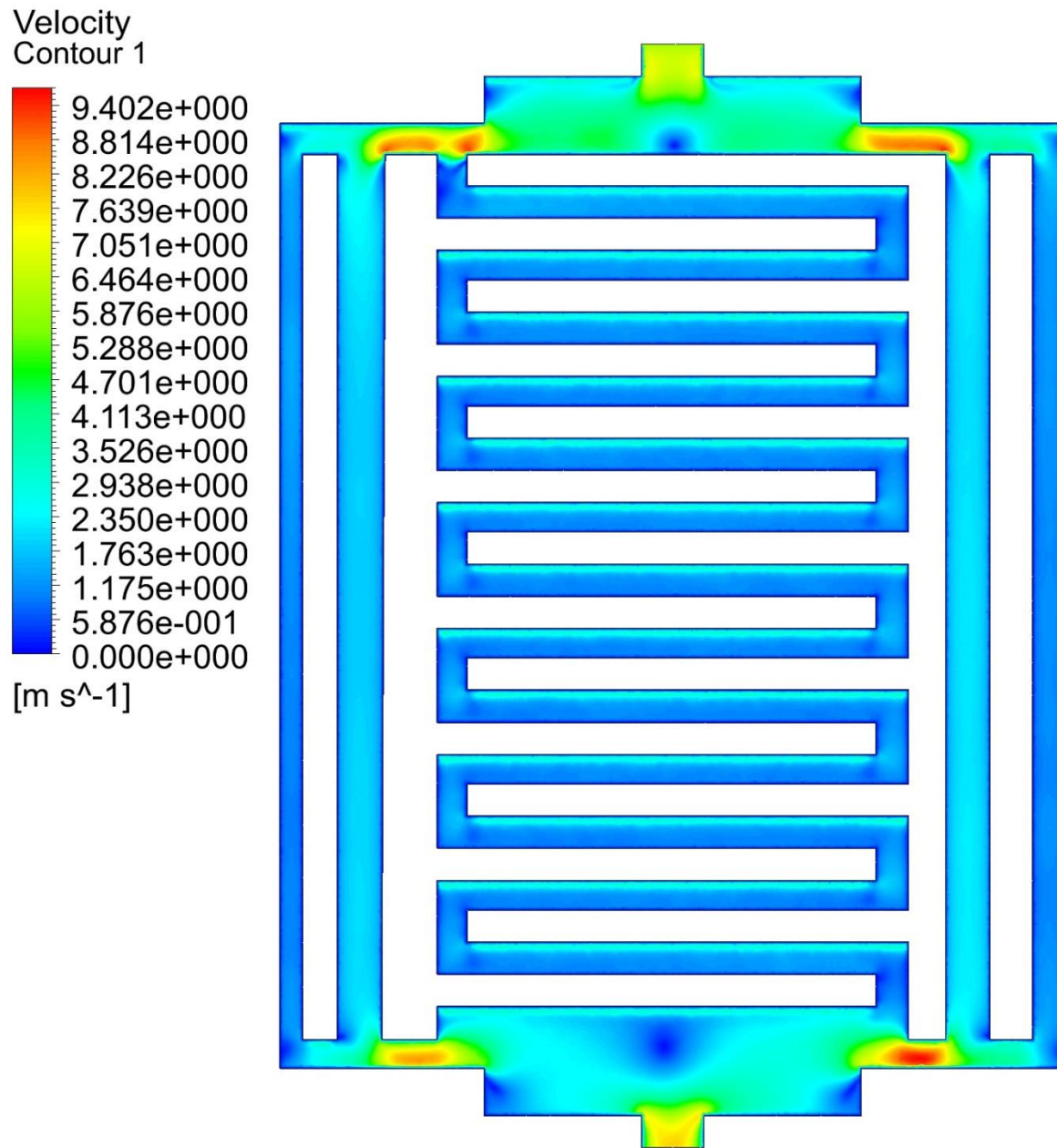


Fig. 28b: Numerical simulation results of the modified Serpentine flow design with 4 by pass channels - Velocity (m/s)

Modification of the Parallel flow plate design

Modification Approach

The main concept is to symmetrically align the inlet and outlet and to create a temporal storage section right on top of the flow channels before the gases are distributed through the channels in a process similar to the concept used in diesel injection systems. This temporal area aid in the uniform distribution of the gases though the flow rates likely to be experienced within the mid region directly opposite to the feed point will be greater. Fig. 29 shows the funnel-like conical shape design that will be integrated into the design.

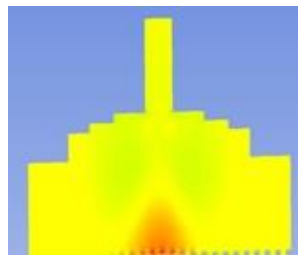


Fig. 29: Temporal conical shape storage design right on top of the channel designs

With the exception of this modification of the inlet area, the design is almost the same as the usual parallel design. The major modification is at the inlet and outlet where the gas is allowed to develop a more even inlet pressure field over the channels inlet points to provide uniform pressure drops and velocity profiles in all the parallel channels.. The design aids in the easy removal of water that may be formed in the channels and also support the even distribution of the gases through these channels.

The mesh used in this simulation is a fine grid of 7,602,020 elements as shown in Fig. 30.

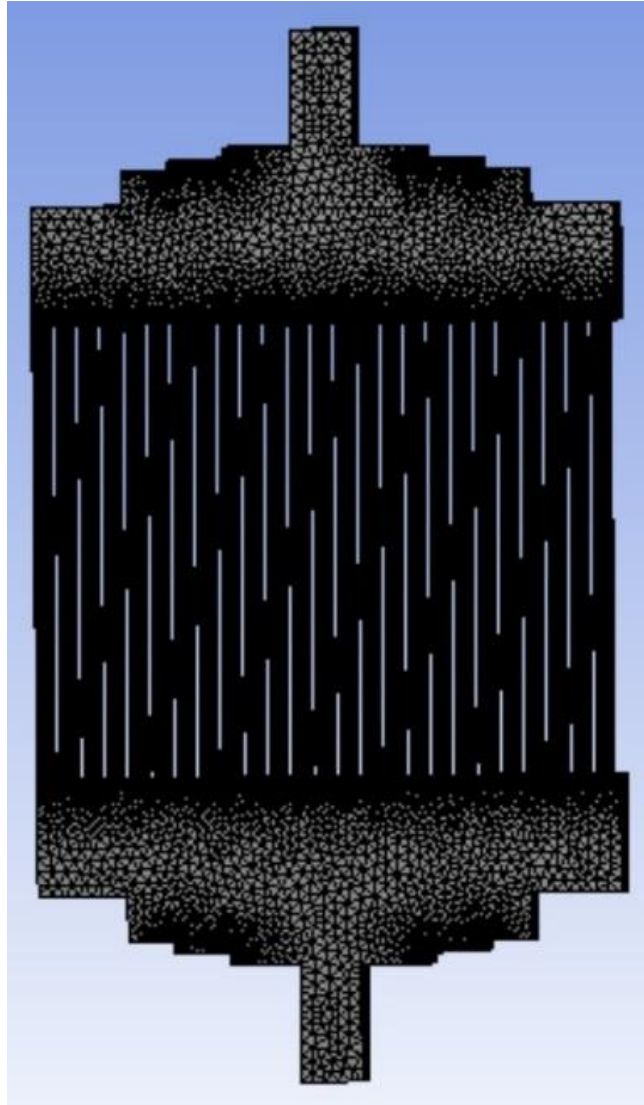


Figure 30: 3-D Straight channel model for meshing of the modified Parallel flow plate.

The pressure distribution profile shown in Fig. 31 indicate that the modified parallel flow plate has a high inlet pressure of 36 Pa and an outlet pressure of 2 Pa with a more uniform pressure distribution throughout the plate. The velocity contour shows uniform velocities in the channel because of the modifications implemented in the flow plate design when compared with the traditional parallel flow plate design.

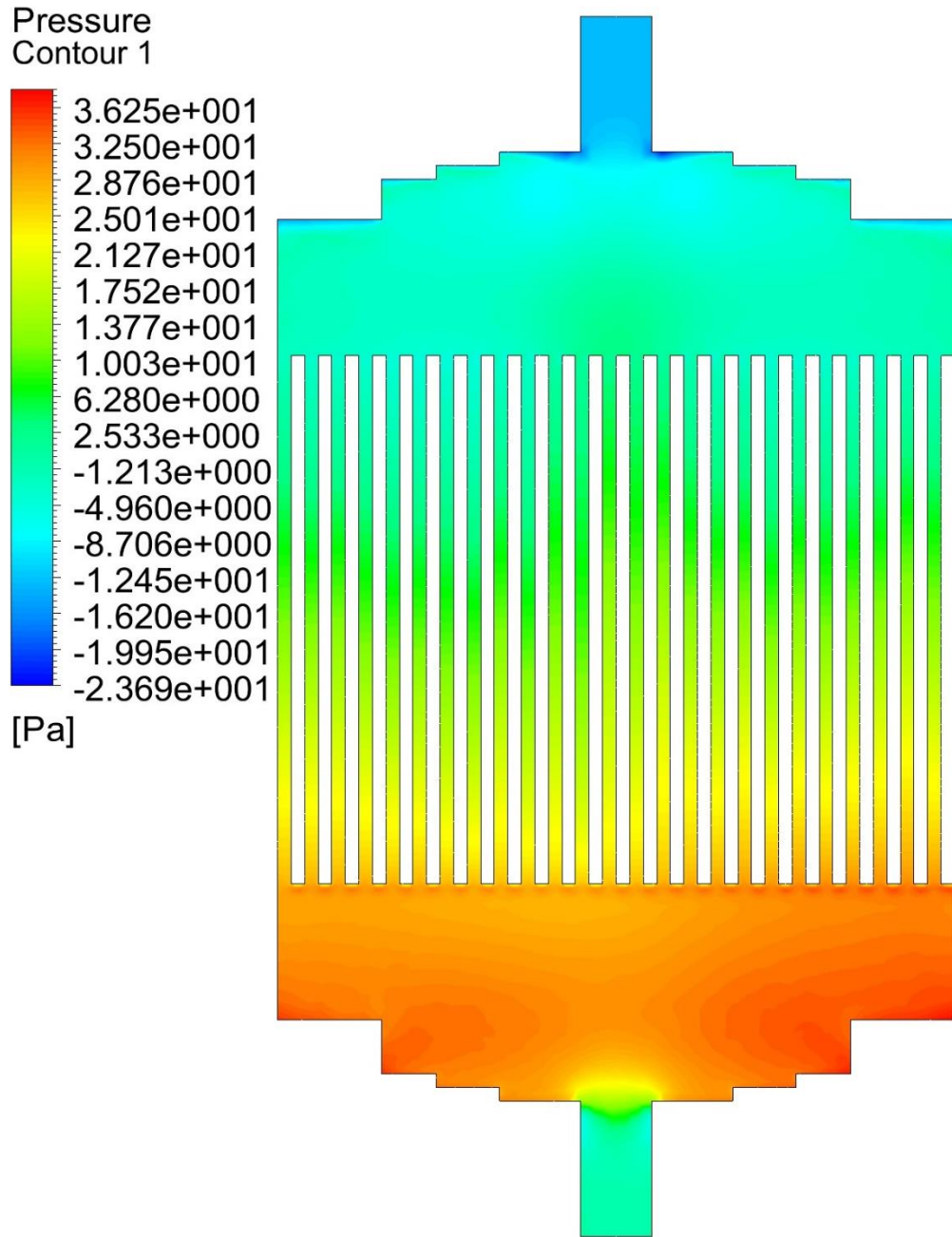


Fig.31a: Numerical simulation results of Parallel flow plates - Pressure distribution (Pa)

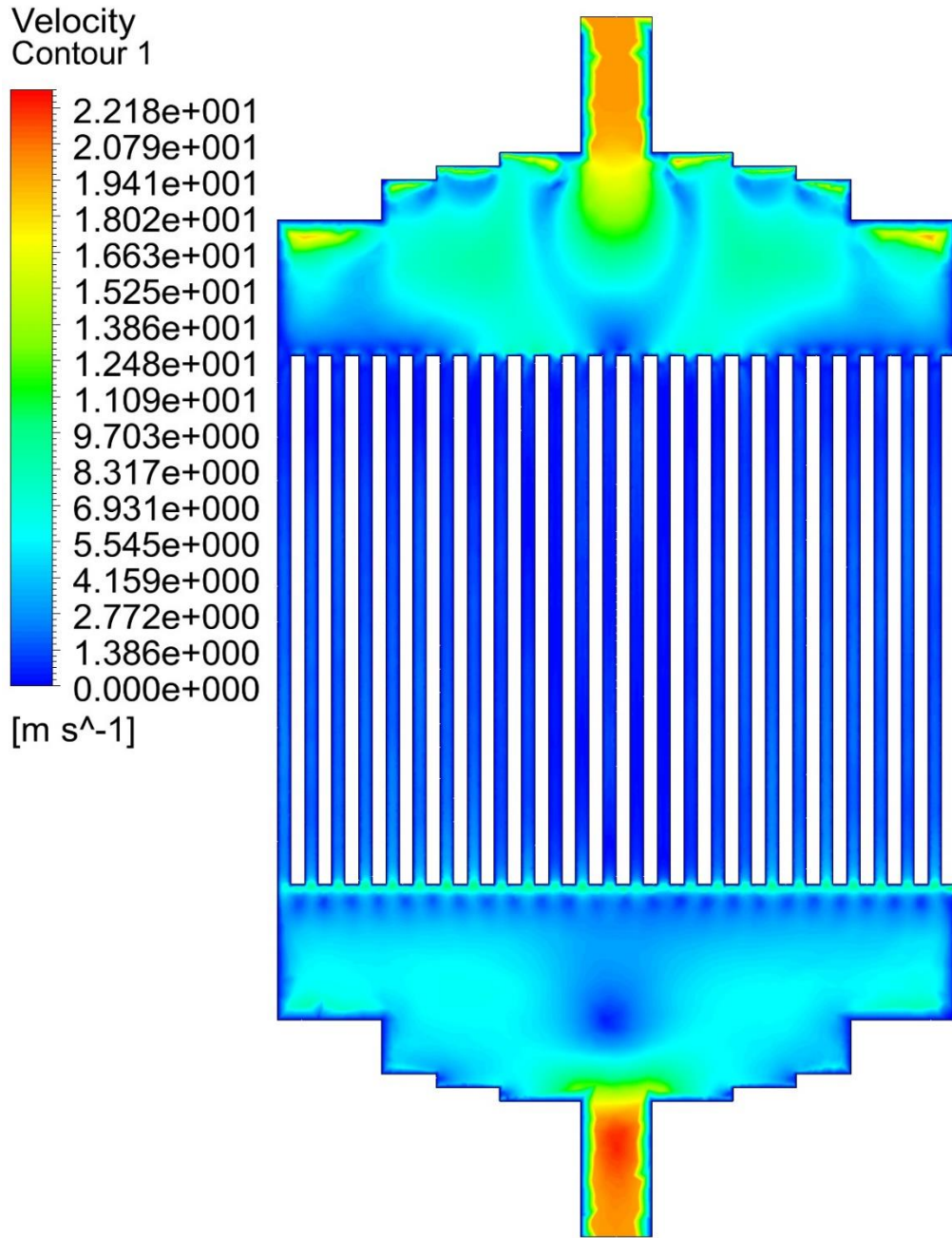


Fig.31b: Numerical simulation results of Parallel flow plates - Velocity (m/s)

Modified Pin Flow Plate design

The modified Pin flow plate design was modelled to have an inject-like structure at the inlet and outlet of the fluid domain where there would be an even distribution of gases throughout the various channels of the fluid domain. The main aim of the modification is to improve the uniformity of the inlet pressure as well as the general distribution of the gas and the MEA. The mesh resulted in 300,225 nodes and 1,324,321 elements as shown in Fig.32.

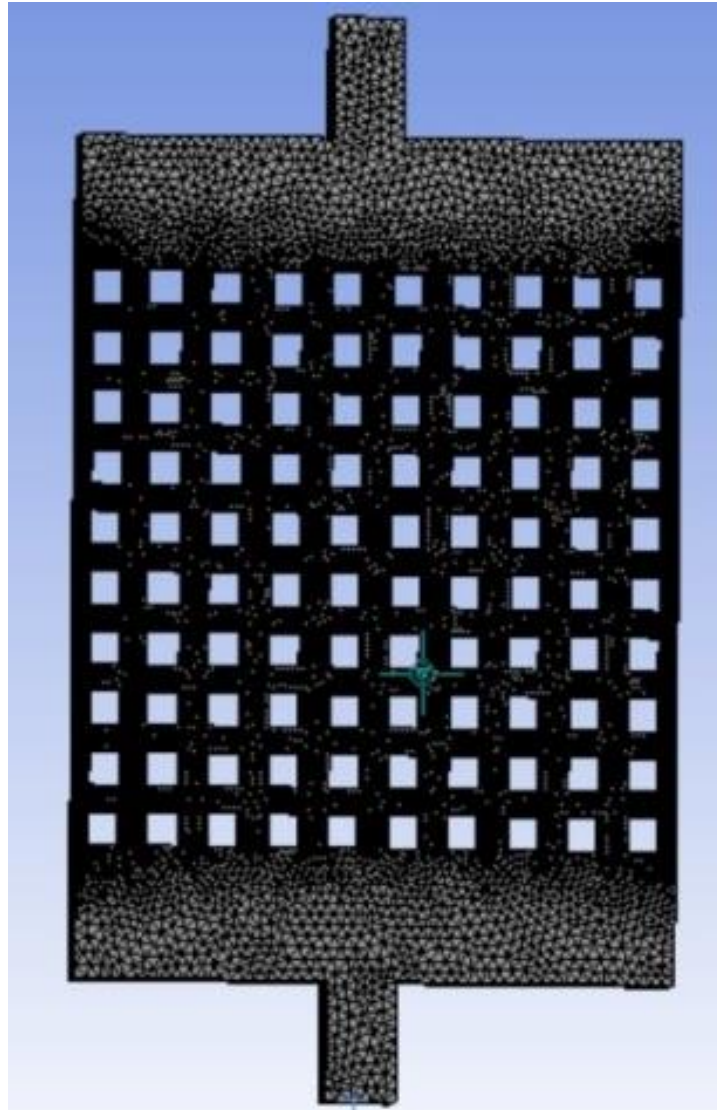


Figure 32: 3 -D Straight channel model of meshing of modified Pin flow plate.

The modified Pin flow plate has a fairly high inlet gauge pressure of 49 Pa and outlet gauge pressure of 2 Pa as shown in Fig. 33a. The pressure drop is even across the mid region. The

velocity profile in Figure 33b shows an outlet velocity that is higher than the inlet velocity due to the volumetric expansion of the gas as the pressure drops. It can also be seen that the low velocity regions formed during the simulation for the modified pin flow plate are smaller compared with the traditional pin flow plate. These low velocity regions are often the dead zones that lead to the accumulation of water which in turn affects the general performance of the fuel cell. The modified plate will therefore increase the efficiency of the fuel cell when compared to the traditional fuel cell.

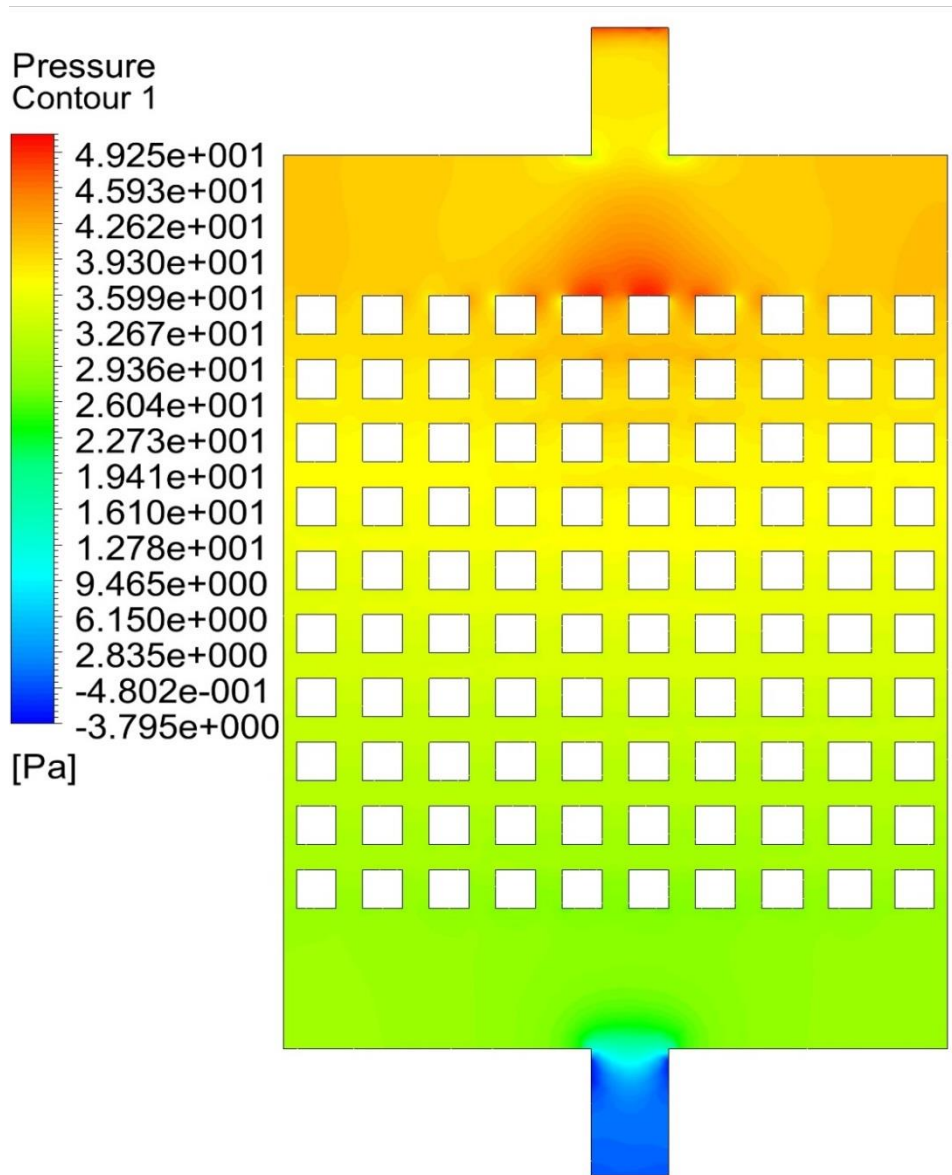


Fig.33a: Numerical simulation results of Pin flow plates - Pressure distribution (Pa)

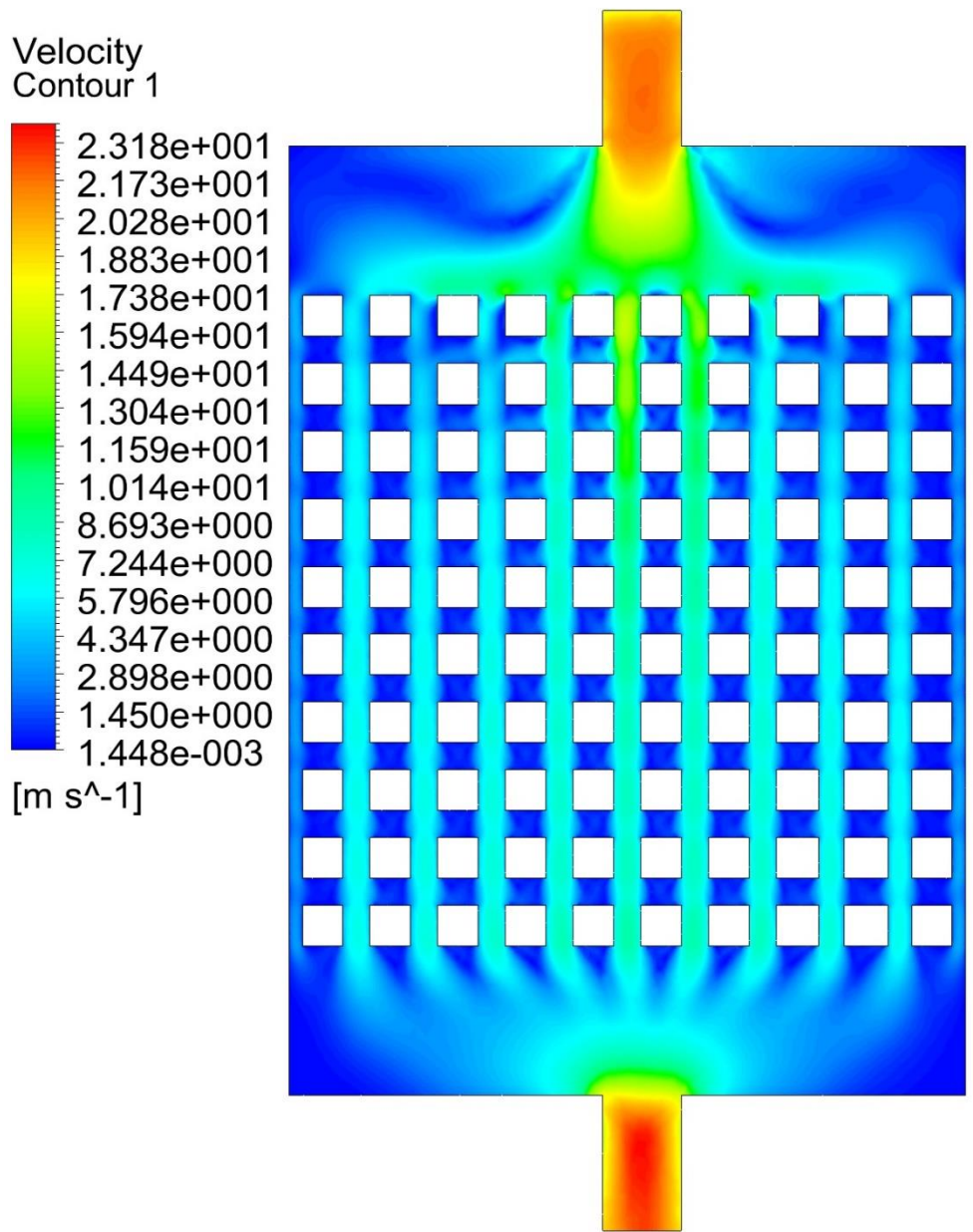


Fig.33b: Numerical simulation results of Pin flow plates - Velocity (m/s)

Further modification of the Pin flow plate: Maze flow plate design

The main goal of this design is to reduce the dead zones inside the plate as gases flow through it. It was also designed with the intension of maximising contact with the gas diffusion layer to reduce the possibility of ohmic resistance and provide improved water removal from the plate while maintaining even gases distribution and pressure against the GDL. A central divergence obstacle was introduced within the central portion of the cell as shown in Fig. 34 during the design phase to improve the distribution of the fluid and to address the need for large contact area. There is the possibility of heat build-up in the central region and consequently this design will work efficiently in single cells with the central contact area increased but it will be very difficult to create a bipolar version of the plate due to the difficulties involved in removing the heat generated.

The mesh created for this simulation included 259503 nodes and 1241691 elements as shown in Fig. 35.

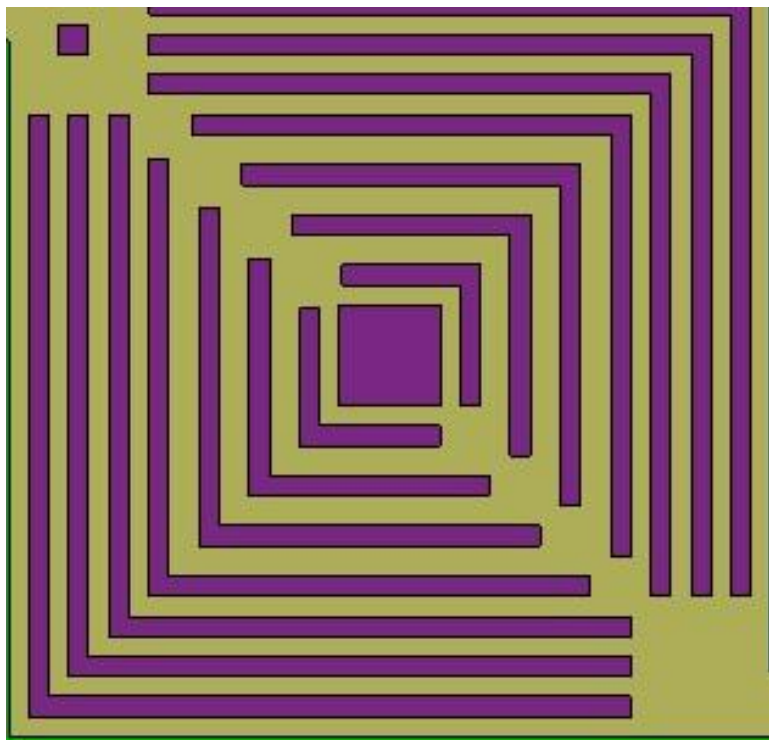


Figure 34: Maze flow design

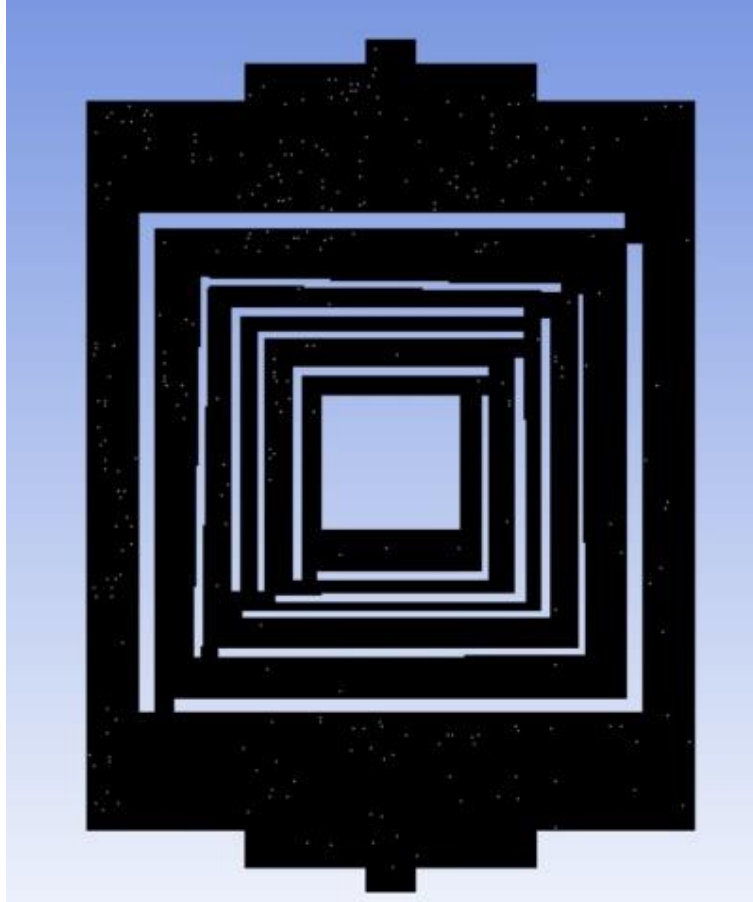


Figure 35: 3-D Straight channel model for meshing of maze flow plate design.

As expected, the outer flow channel can be seen to have a higher pressure compared to that of the inner channel, Fig. 36a. The pressure difference between these channels is what would eventually drive the water droplet that will be formed in the fuel cell out. There is a large pressure drop from the inlet to the outlet but this pressure is not evenly distributed within the flow field. This will have a negative impact on the general performance of the fuel cell with non-uniform performance over the catalyst area. Some of these impacts are dehydration of the membrane and GDL which will finally lead to the damage of the MEA.

Pressure
Contour 1

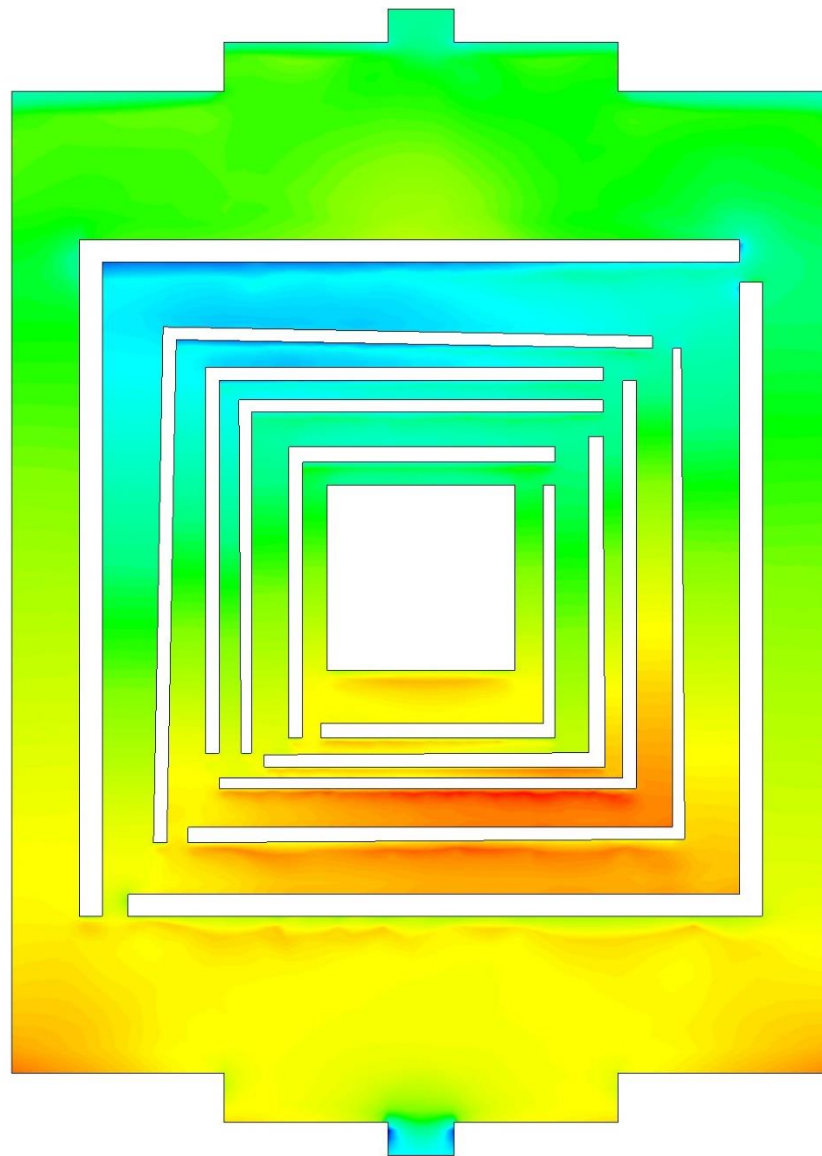
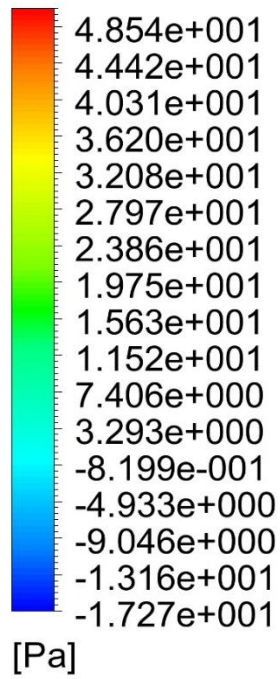


Fig.36a: Numerical simulation results of Maze flow plates - Pressure distribution (Pa)

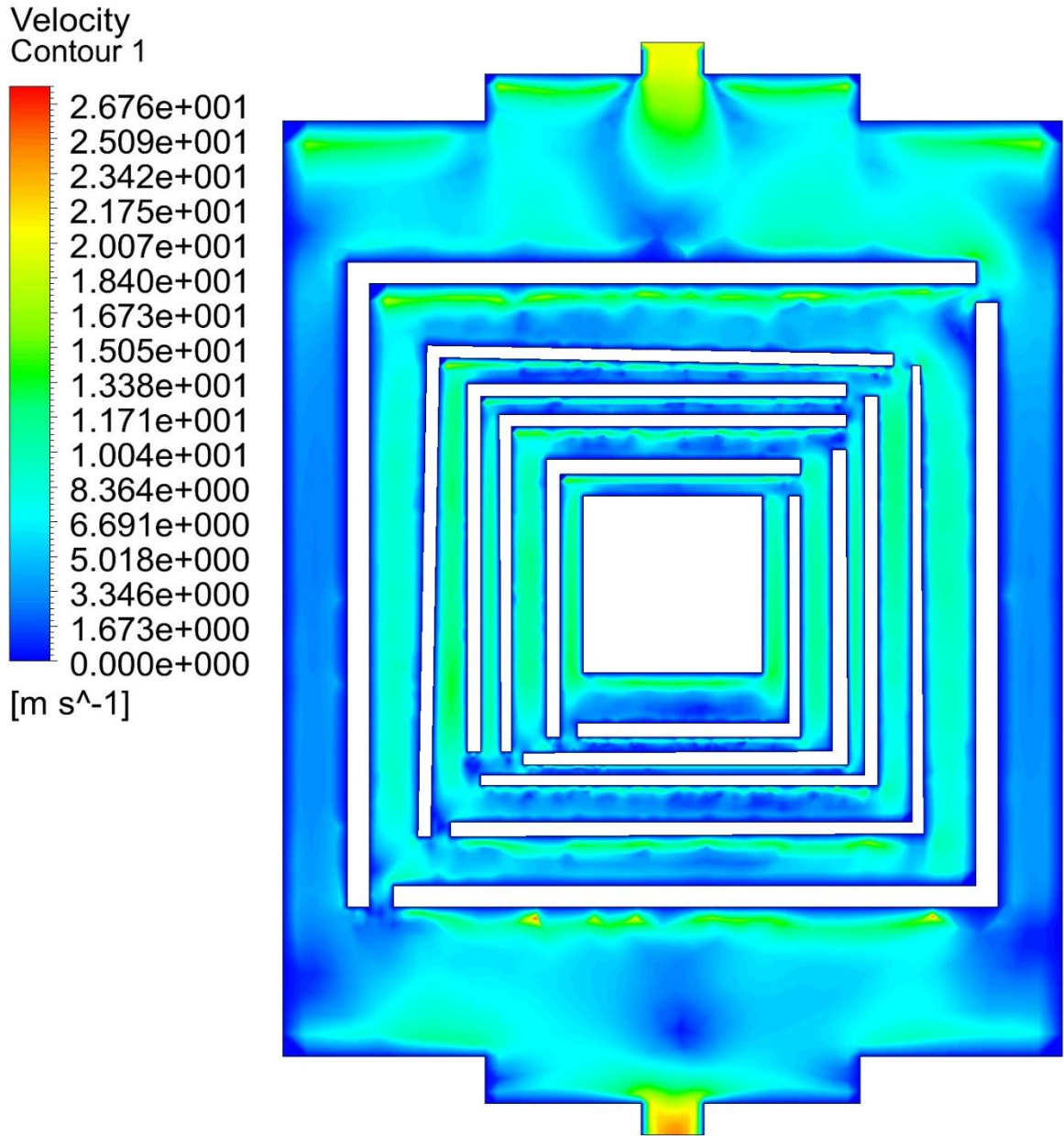


Fig.36b: Numerical simulation results of Maze flow plates - Velocity (m/s)

The velocity distribution within the flow field is shown in Fig. 36b which indicates that the fluid is flowing uniformly within the mid region of the plate. The inlet region has a gap included in the design to promote even distribution of the gases throughout the central part of the design.

Optimisation of modified flow plates designs

As already indicated earlier, the main purpose of this work is the consideration of one aspect of the performance characteristics of fuel cells which is the pressure drop in the flow channels. Previous figures showed the pressure contours for different flow plate designs of commonly used cells and also the corresponding pressure contours for the modified designs. Figs. 37 to 40 show the effect of flow rate or velocity on the pressure drop in the flow channels of the suggested modified designs. Comparing this with simulation and published data it can be demonstrated that all modified designs resulted in lower pressure drops than the respective original designs for the selected velocity ranges.

Pressure drop profile for Serpentine flow plate channel designs

Fig. 36 shows the pressure drops for serpentine channel, modified serpentine plate with 2 bypass channels and the modified serpentine plate with 4 bypass channels over a range of velocities. It can be seen that the modified serpentine designs has significantly lower pressure drop, approximately 50 times lower than that of the traditional serpentine design. It can also be observed that introducing 4 bypass channels instead of 2 bypass channels in the modified serpentine design, reduces the pressure drop by over 50%. At 12m/s the pressure drop is approximately 30Pa for 4 bypass channels serpentine design and that of 2 bypass channels serpentine design is 100Pa showing massive difference between the two designs.

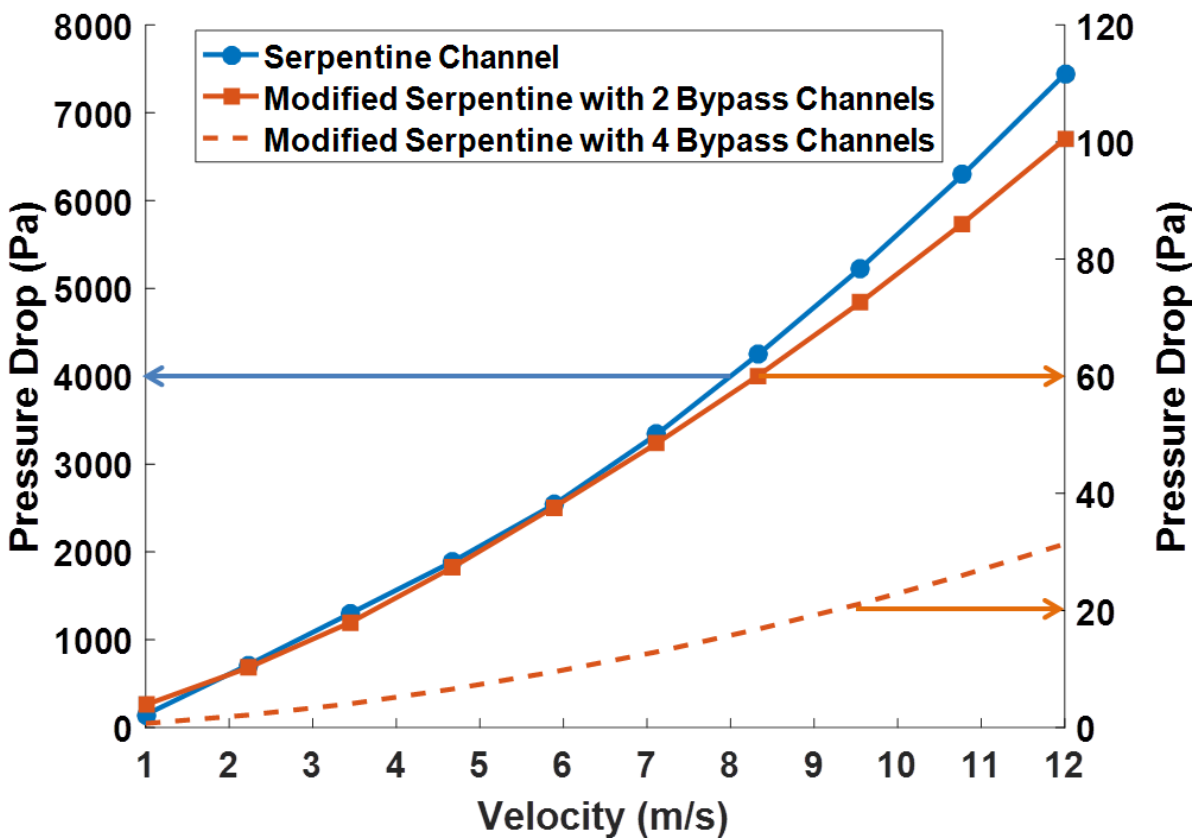


Fig. 37: A plot of velocity against pressure drop for traditional and modified serpentine flow plate designs

Pressure drop profile for parallel flow plate designs

The pressure drop profile from Fig. 38 shows the effect of the modified parallel channel design compared with the traditional parallel design. The pressure drop for the traditional parallel design is 90 Pa at a velocity of 12 m/s while that of the modified design is 15 Pa. This huge difference is due to the diesel injection-like design introduced at the inlet and outlet of the traditional parallel design as shown in Fig. 29. This modification allows the gas to flow more uniformly through the channels avoiding the development of high pressure region near the dead end of the gas feed region.

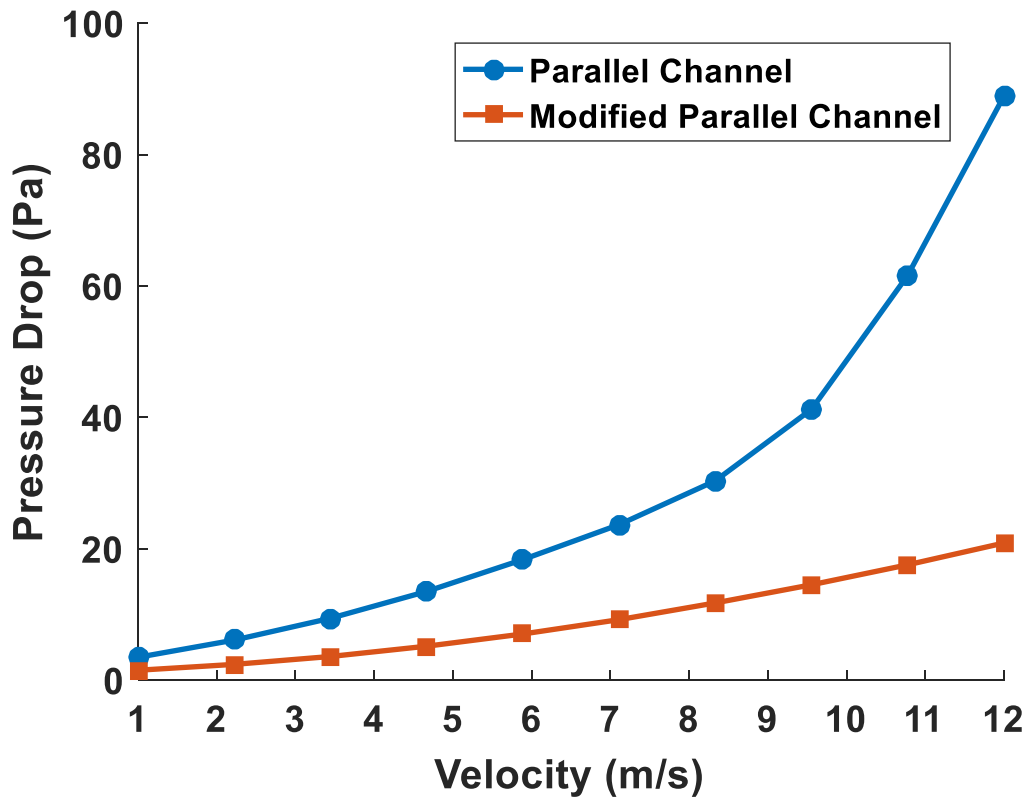


Fig. 38: A plot of velocity against pressure drop for parallel and modified parallel flow plates

Pressure drop profile for modified Pin and Maze flow plate designs

From Fig. 39, the pressure drop for the modified pin flow plate design was less compared to the new maze flow plate design. The pin flow plate design will be a better option to improve the performance of the fuel cell with respect to pressure drop compared to the maze design for the whole velocity range as shown in the Fig. 39.

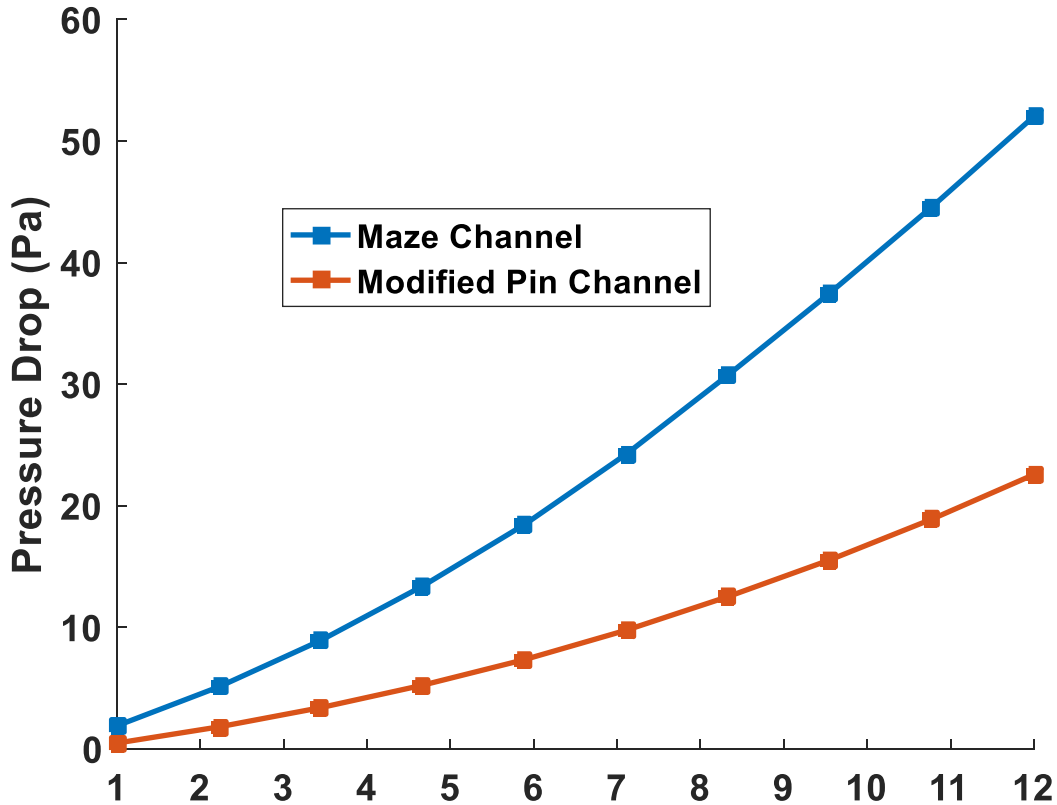


Fig. 39: A plot of velocity against pressure drop for modified Pin flow plates

Pressure drop profile for all modified flow plate designs

Fig. 40 shows the comparison of pressure drop profiles for the different modified flow plate designs. As expected the modified serpentine design with the 2 bypass channels developed higher pressure drop compared with the rest of the modified designs. It is also observed that the modified parallel and pin flow channel designs displayed the lowest pressure drops for the 5cm x 5cm plates. The implication of this is that the two designs may result in reduced construction and compression costs, but the overall performance improvement will be a combination of the effect of the pressure drop as well as other factors such as temperature, humidity, stoichiometry, etc.

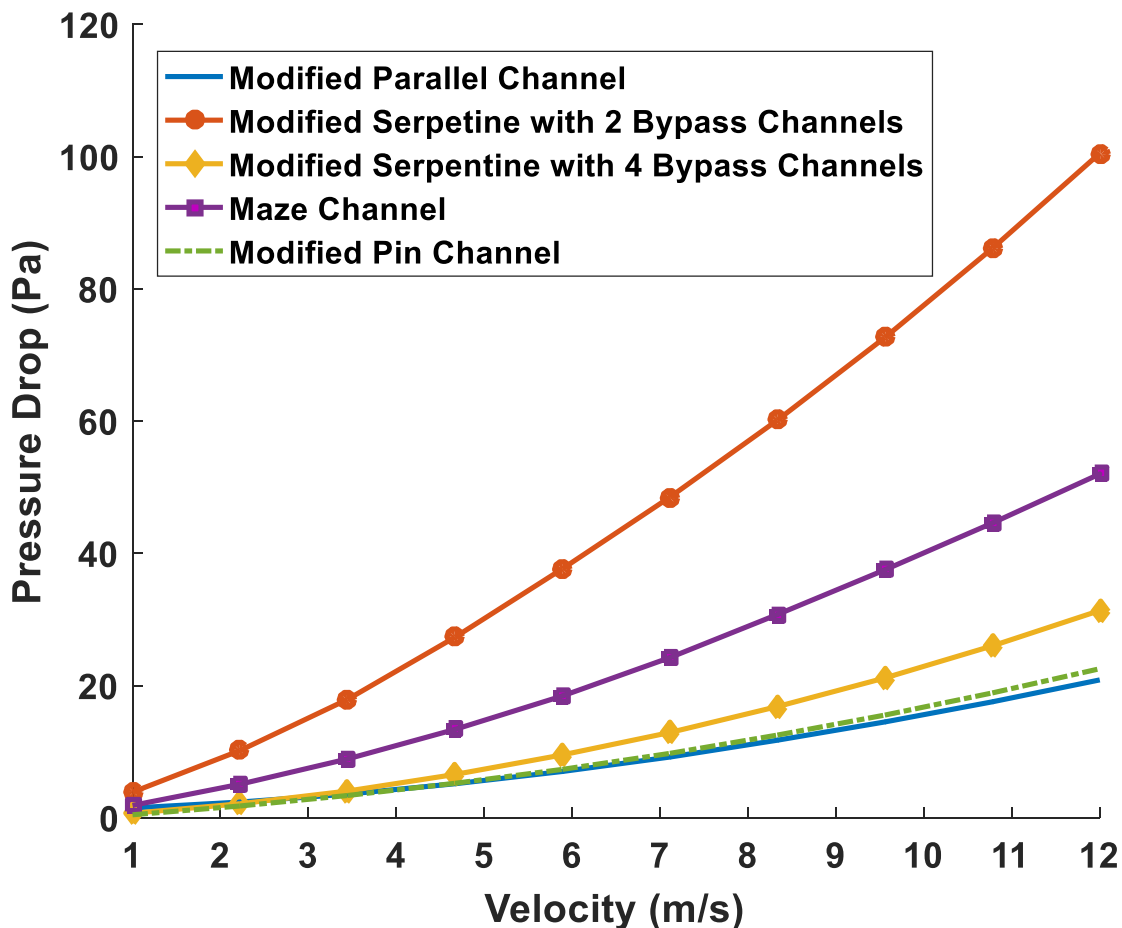


Fig. 40: A plot of velocity against pressure drop for all modified flow plate designs

Conclusion

An in-depth literature review of the various types of fuel cell flow plates was conducted with advantages and disadvantages of the commonly used types investigated. Using a set plate size of a square of 5cm X 5cm, the flow in several of these common types were simulated using ANSYS CFX and the resultant pressure drops in the plates were calculated.

New flow plate designs were developed by modifying of the existing flow plate designs and optimised using ANSYS CFX to study the effect of the modifications on the plates pressure drops. This was extended further to compare the designs at different flow rates (inlet velocities) and the impact on pressure drop profiles. The results obtained for most of the modified designs showed reduction in pressure drop which impacts positively on the overall performance of the fuel cell. Mesh convergence studies were carried out at the onset to ensure there were no results dependencies on the mesh used for the simulation.

A combination of both the serpentine and the parallel flow channels was designed to achieve a better performance resulting from the presence of the serpentine channel portion and at the same time ensure overall lower pressure drop due to the presence of the parallel bypass channels. From the simulation results it has been identified that the modified serpentine designs with bypass channels provided a pressure drop of 50 times lower than the traditional serpentine design.

Moreover, the modified parallel flow channel achieved a very low pressure drop at 12m/s with an overall reduction of 90% to that of the traditional parallel channel.

The new maze flow plate design compared with that of the modified pin channel however had approximately 40% high pressure drop at 12m/s.

Compared with all of the modified designs, the modified parallel flow channel has the lowest pressure drop.

This study was restricted to pressure drop in fuel cell flow plate design that are commonly referenced in the literature and modified them to achieve lower pressure drops. The overall performance of any particular fuel cell is dependent on many other factors in addition to the pressure drop and further studies need to be carried out to explore the interaction between these different parameters and their combined effect on a fuel cell performance.

Finally, this simulation investigation seeks to initiate future developments in novel fuel cell plate designs that can help overcome some of the current problems and provide better solutions to improve the fuel cell efficiencies and accelerate their uptake in different applications including the automotive industry.

References

1. J.G. Carton and A.G. Olabi, Design of experiment study of the parameters that affect performance of three flow plate configurations of a proton exchange membrane fuel cell, *Energy*, 35 (7), pp 2796-2806, 2010.
2. Tabbi Wilberforce, A. Alaswad, A. Palumbo, A. G. Olabi, Advances in stationary and portable fuel cell applications, *International Journal of Hydrogen Energy* 41(37) March 2016.
3. J. G. Carton and A. G. Olabi, Representative model and flow characteristics of open pore cellular foam and potential use in proton exchange membrane fuel cells, *International Journal of Hydrogen Energy* 40 (2015) 5726 – 5738.
4. A. G. Olabi, The 3rd international conference on sustainable energy and environmental protection SEEP 2009 the guest editor's introduction, *Energy* 2010; 35:4508-9.
5. Li Xianguo, *Principles of Fuel Cells*, 2006, New York: Taylor and Francis group.
6. C. Spiegel, 2007, *Designing and Building Fuel Cells*. 1st ed. McGraw-Hill Professional.
7. Fuel cells. Energy Research Center of the Netherlands (ECN).
<http://www.ecn.nl/en/h2sf/additional/fuel-cells-explained/>. (Accessed: 04/11/2016).
8. T. Wilberforce, A. Al Makky, A. Baroutaji, R. Sambhi, A.G. Olabi, Computational Fluid Dynamic Simulation and modelling (CFX) of Flow Plate in PEM fuel cell using Aluminum Open Pore Cellular Foam Material, *Power and Energy Conference (TPEC)*, IEEE, Texas. 2017. DOI: 10.1109/TPEC.2017.7868285.
9. S. K. Dong, B. T. Yun and D. K. Lee, Design and numerical study for 1 kW tubular SOFC APU system. Anonymous Fuel Cell Seminar, San Antonio; TX; United states: Electrochemical Society Inc, October 2007, pp- 701-706.
10. NASA, 2015. Summary: Space Applications of Hydrogen And Fuel Cells.
http://www.nasa.gov/topics/technology/hydrogen/hydrogen_2009.html (Accessed: 10/07/2017)
11. J. Larminie and A. Dicks, *Fuel Cell System Explained*. 2nd edition, 2003, Wiley-Blackwell.
12. V. S. Bagotsky, *Fuel Cells: Problems and Solutions*, 2009, Wiley.
13. M. A. Peavey, In: *Fuel from water: energy independence with hydrogen*. 11th ed. Louisville, KY: Merit Inc: 2003.

14. T. Wilberforce, Z. El-Hassan, F.N. Khatib, A. Al Makyy, A. Baroutaji, J. G. Carton and A. G. Olabi, Modelling and Simulation of Proton Exchange Membrane Fuel cell with Serpentine bipolar plate using MATLAB, International journal of hydrogen, 2017. DOI: 10.1016/j.ijhydene.2017.06.091.
15. B. Cook, Introduction to fuel cells and hydrogen technology, Eng. Sci. Educ. J., 2002; 11(6): 205 – 16.
16. S. Superamian, Fuel Cells: from fundamentals to applications, New York: Springer Science & Business Media: 2006.
17. H. Tsuchiya H and O. Kobayashi. Mass production of PEM fuel cell by learning curve., International Journal on Hydrogen Energy 2004; 29:985 – 90.
18. H. P. Chang, C. L. Chou, Y. Chen, T. Hou and B. J. Weng, The design and cost analysis of a portable PEMFC UPS system, International Journal on Hydrogen Energy 2007; 32:316 – 22.
19. T. Wilberforce, A. Al Makky, A. Baroutaji, R. Sambhi and A.G Olabi, Optimization of bipolar plate through computational fluid dynamics simulation and modelling using nickle open pore cellular foam material, International conference on renewable energies and power quality (ICREPQ'17), ISSN 2171-038X, No 15 April 2017.
20. E. Afsari and S. A. Jazayeri, Effects of the cell thermal behavior and water phase change on a proton exchange membrane fuel cell performance, Energy Convers Manage 2010; 51: 655 – 62.
21. A. D. Le and B. Zhou, A generalized numerical model for liquid water in a proton exchange membrane fuel cell with interdigitated design, J. Power Sources ,193 (2), pp 665683,2009.
22. A. Kazim, H. T. Liu and P. Forges, Modelling of performance of PEM fuel cells with conventional and interdigitated flow fields, J. Appl. Electrochem., 29 (12), pp 1409-1416,1999.
23. J. P. Kloess, X. Wang, J. Liu, Z. Shi and L. Guessous, Investigation of bio-inspired flow channel designs for bipolar plates in proton exchange membrane fuel cells, J. Power Sources, 188(1), pp 132-140, 2009.

24. T. Wilberforce, A. Alaswad, J. Mooney and A. G. Olabi, Hydrogen Production for Solar Energy Storage. A Proposed Design Investigation, Proceedings of the 8th International Conference on sustainable Energy and Environmental Protection. ISBN: 978-1-903978-52-8. 2015.
25. Y. G. Yoon, W. Y. Lee, G. G. Park, T. H. Yang and C. S. Kim, Effects of channel and rib widths of flow field plates on the performance of a PEMFC, International Journal Hydrogen Energy 2005; 30:1363 – 6.
26. X. D. Wang, W. M. Yan, Y. Y. Duan, F. B. Weng, G. B. Jung and C. Y. Lee, Numerical study on channel size effect for proton exchange membrane fuel cell with serpentine flow field, Energy convers Manage 2010; 51:959 – 68.
27. A. Su, F. B. Weng, C. Y. Hsu and Y. M. Cheng, Studies on flooding in PEM fuel cell cathode channels, International Journal Hydrogen Energy 2006; 31:1031 – 9.
28. M. Venkatraman, S. Shimpalee, J. W. Van Zee, S. I. Moon and C. W. Extrand, Estimates of pressure gradients in PEMFC gas channels due to blockage by static liquid drops, International Journal Hydrogen Energy 2009;34:5522 – 8.
29. A. P. Manso, F. F. Marzo, J. Barranco, X. Garikano, and M. Garmendia Mujika, Influence of geometric parameters of the flow fields on the performance of a PEM fuel cell. A review, International Journal of Hydrogen Energy, 37 (20), pp 15256-15287, 2012.
30. H. F. Zhang, P. C. Pei and X. Yuan, The conception of in – plate adverse – flow field for a proton exchange membrane fuel cell, International Journal Hydrogen Energy 2010; 35:9124 – 33.
31. M. Z. Yazdi and M. Kalbasi, A novel analytical analysis of PEM fuel cell, Energy convers Manage 2010; 51:241 – 6.
32. W. M. Yan, H. C. Liu, C. Y. Soong, F. Chen and C. H. Cheng, Numerical study on cell performance and local transport phenomena of PEM fuel cells with novel flow field designs, Journal Power Sources 2006; 161:907 – 19.
33. X. D. Wang, Y. Y. Duan, W. M. Yan, D. J. Lee, A. Su and P. H. Chi, Channel aspect ratio effect for proton exchange membrane fuel cell with serpentine flow field: role of sub – rib convection, Journal Power Sources 2009; 193: 684 – 90.

34. C. J. Tseng, B. T. Tsai, Z. S. Liu, T. C. Cheng, W. C. Chang and S. K. Lo, A PEM fuel cell with metal foam as flow distributor, *Energy Conversion and Management* 62 (2012): 14-21.
35. C.J. Tsang, B.T. Tsai, Z.S. Liu, T.C. Cheng, W.C. Chang and S.K. Lo, Effects of flow field design on the performance of a PEM fuel cell with metal foam as the flow distributor, *International Journal of Hydrogen Energy*, 37 (17), pp 13060-13066, 2012.
36. A. Kumar and R.G. Reddy, Materials and design development for bipolar/end plates in fuel cells, *J Power Sources*, 129 (1), pp 62-67, 2004.
37. H. Liu and P. Li, Even distribution/dividing of single-phase fluids by symmetric bifurcation of flow channels, *International Journal of Heat and Fluid Flow*, 40, pp 165-179, 2013.
38. H. Liu, P. Li and J.V. Lew, CFD study on flow distribution uniformity in fuel distributors having multiple structural bifurcations of flow channels, *International Journal of Hydrogen Energy*, 35 (17), pp 9186-9198, 2010.
39. G. M. Imbrioscia and H. J. Fasoli, Simulation and study of proposed modifications over straight-parallel flow field design, *International Journal of Hydrogen Energy*, 39 (16), pp 8861-8867 (2014).
40. E. Hontanon, M. J. Escudero, C. Bautista, P. L. GarciaYbarra and L. Daza, Optimisation of flow-field in polymer electrolyte membrane fuel cells using computational fluid dynamics techniques, *Journal of Power Sources*, 86(1), pp 363368, 2000.
41. M. Mohammadi, G. N. Jovanovic and K.V. Sharp, Numerical study of flow uniformity and pressure characteristics within a microchannel array with triangular manifolds, *Computers & Chemical Engineering*, 52, pp 134144, 2013.
42. A. Lozano, L. Valiño, F. Barreras and R. Mustata, Fluid dynamics performance of different bipolar plates: Part II. Flow through the diffusion layer, *Journal of Power Sources*, 179 (2), pp 711–722, 2008.
43. F. Barreras, A. Lozano, L. Valiño, C. Marín and A. Pascau, Flow distribution in a bipolar plate of a proton exchange membrane fuel cell: experiments and numerical simulation studies, *Journal of Power Sources*, 144 (1), pp 54–66, 2005.